European Journal of Taxonomy 943: 239–287
https://doi.org/10.5852/ejt.2024.943.2599
ISSN 2118-9773
www.europeanjournaloftaxonomy.eu
2024 · Chen H.-P. *et al.*

Research article
urn:lsid:zoobank.org:pub:4EEAB64C-EB8D-4208-9EE2-76FA07201EED

Integrative taxonomy reveals unanticipated hidden diversity in the monotypic goosefish genus *Lophiomus* (Teleostei, Lophiidae), with description of three new species and resurrection of *Chirolophius laticeps* Ogilby, 1910

Hsuan-Pu CHEN [1], Mao-Ying LEE [2] & Wei-Jen CHEN [3,*]

[1]Department of Entomology, National Taiwan University, No.1, Sec. 4, Roosevelt Road, Taipei 10617, Taiwan.
[2]Marine Fisheries Division, Fisheries Research Institute, Ministry of Agriculture, No. 199 Hou-Ih Road, Keelung 202008, Taiwan.
[3]Institute of Oceanography, National Taiwan University, No.1, Sec. 4, Roosevelt Road, Taipei 10617, Taiwan.

*Corresponding author: wjchen.actinops@gmail.com
[1]Email: pooh890510@gmail.com
[2]Email: coleopetera@gmail.com

[1]urn:lsid:zoobank.org:author:CA33BB9B-9BDC-4497-9768-AD750874E7C4
[2]urn:lsid:zoobank.org:author:761CF9F8-ABD7-4DA5-9326-D4160526731C
[3]urn:lsid:zoobank.org:author:4D399FDB-F893-422E-A8A2-ACC18F40FCFD

Abstract. Thought to be monotypic for decades, the only species in the goosefish genus *Lophiomus* Gill, *Lm. setigerus* (Vahl), shows a wide range of morphological variation and is distributed widely in the Indo-West Pacific (IWP). In this study, datasets for two mitochondrial and two nuclear genes sequences obtained from samples of *Lophiomus* collected in different localities across the IWP were constructed and analyzed to explore the phylogeny and species diversity within the genus. Our integrated approach with multiline evidence unveiled an unanticipated richness of at least six delimited species of *Lophiomus*. Herein, based on materials already available from museums and new specimens obtained primarily through the *Tropical Deep-Sea Benthos* program surveying IWP benthic fauna, we formally describe three new species: *Lm. immaculioralis* sp. nov., *Lm. nigriventris* sp. nov., and *Lm. carusoi* sp. nov. Also, we resurrect *Lm. laticeps* stat. rev. from synonyms of *Lm. setigerus*. These species can be diagnosed by genetics, body coloration, patterns on the floor of the mouth, peritoneum pigmentation, morphometric measurements, and meristic counts of cranial spines, dorsal-fin spines, and pectoral-fin and pelvic-fin rays from each other and from *Lm. setigerus*. The species *Lm. setigerus*, as well as the genus *Lophiomus*, are re-described accordingly based on the new results. Amended identification keys to the four extant lophiid genera and to species of *Lophiomus* are also provided.

Keywords. Biodiversity, Indo-West Pacific, anglerfish, multigene phylogeny, species delimitation, Tropical Deep-Sea Benthos.

Chen H.-P., Lee M.-Y. & Chen W.-J. 2024. Integrative taxonomy reveals unanticipated hidden diversity in the monotypic goosefish genus *Lophiomus* (Teleostei, Lophiidae), with description of three new species and resurrection of *Chirolophius laticeps* Ogilby, 1910. *European Journal of Taxonomy* 943: 239–287. https://doi.org/10.5852/ejt.2024.943.2599

Introduction

The anglerfish family Lophiidae Rafinesque, 1810 is composed of medium- to large-sized teleosts living generally on sandy and muddy bottoms of the continental shelf and continental slope in the deep sea (Pietsch 1984, 2009; Miya *et al.* 2010). Commonly known as goosefishes, they feature relatively large heads with wide mouths and dorsoventrally compressed bodies that are well adapted to their benthic lifestyle (Pietsch 1984, 2009). The family comprises four extant genera: *Lophius* Linnaeus, 1758, *Lophiomus* Gill, 1883, *Lophiodes* Goode & Bean, 1896, and *Sladenia* Regan, 1908, altogether comprising 29 recognized species found in the Arctic, Atlantic, Indian, and Pacific Oceans (Caruso 1981, 1983, 1985; Leslie & Grant 1991; Ho *et al.* 2011, 2014; Ni *et al.* 2012; Fricke *et al*. 2022). The family also includes three extinct genera: *Eosladenia* Bannikov, 2004, *Sharfia* Pietsch & Carnevale, 2011, and *Caruso* Carnevale & Pietsch, 2012 (Bannikov 2004; Pietsch & Carnevale 2011; Carnevale & Pietsch 2012). Extant genera can be generally delimitated by their habitus and such osteological features as the number of vertebrae, morphology of maxilla and dentary bones, frontal ridges, and neurocranial spines (Caruso 1985). Some lophiid fishes, especially the large species in the genus *Lophius*, are targeted in commercial fisheries in North America, Europe, and Japan (Haring & Maguire 2008). Phylogenetically, Lophiidae is placed as the basal-most lineage of the Lophiiformes Garman, 1899, and the intergeneric relationship of extant lophiid genera is resolved as (*Sladenia*, (*Lophiodes*, (*Lophius*, *Lophiomus*))), which is supported by morphological (Caruso 1985; Carnevale & Pietsch 2012) and molecular evidence (Miya *et al.* 2010).

Lophiomus as a monotypic genus is comprised only of *Lm. setigerus* (Vahl, 1797), which is mainly found in the Indo-West Pacific (IWP) (Caruso 1983). It was originally separated from the genus *Lophius* by a reduced number of vertebrae (18–19 in *Lophiomus* and more than 25 in *Lophius*), but the oversimplified generic definition gave some arguments to classify the species into the three genera of *Lophiomus*, *Lophius*, and *Lophiodes* (Gill 1883; Caruso 1981, 1983). For example, *Lophius litulon* (Jordan, 1902) and several species of *Lophiodes* (*Ld. caulinaris, Ld. miacanthus, Ld. olivaceus* [= *Ld. mutilus*], and *Ld. spilurus*) were originally misplaced in *Lophiomus* due to there being no exhaustive examination of morphological characteristics (Caruso 1981, 1983). Caruso (1983) revised the two morphologically similar genera *Lophiomus* and *Lophius*, and redefined *Lophiomus* by meristic counts of vertebrae, cranial spines, dorsal- and anal-fin rays, dark markings on the floor of mouth, the presence of low conical knobs on the frontal ridge, the outer surface of the maxilla, and dentary bones.

Caruso (1983) also proposed that *Lophius viviparus* Bloch & Schneider, 1801, *Lophius indicus* Alcock, 1889, *Chirolophius laticeps* Ogilby, 1910, *Lophiomus longicephalus* Tanaka, 1918, and *Chirolophius malabaricus* Samuel, 1963 should be synonymized with *Lm. setigerus* based on morphological evidence obtained from his review of original descriptions and type specimen examinations for two of those nominal species (*Lp. indicus* and *C. laticeps*). Those previous nominal species and *Lm. setigerus* present subtle morphological differences in body color pattern, peritoneum pigmentation, and counts of pectoral-fin rays. The differences were considered by the author to represent merely geographical variations, and the distribution of *Lm. setigerus* was thus extended to the whole Indo-West Pacific. However, the taxonomic status of the widely distributed and sometimes phenotypically variable species is often challenged by the results of modern integrated approaches in systematic biology (Dayrat 2005; Borsa *et al.* 2013a, 2013b, 2014; Lee *et al.* 2019; Chen & Borsa 2020). We believe that *Lm. setigerus* as currently defined may present cryptic species diversity.

Thus, the aim of this study is to revise the taxonomy of *Lophiomus* by an integrated approach combining both molecular and morphological analyses on the basis of 35 newly collected, seven museum voucher specimens, and three available type specimens of *Lophiomus* from the IWP. The new materials were collected from six oceanographic expeditions undertaken by the '*Tropical Deep-Sea Benthos* (TDSB)' program (Bouchet *et al.* 2008) and '*Taiwan-France Marine Diversity Exploration and Evolution of Deep-Sea Fauna* (TFDeepEvo 2013–2016)' cooperative research program with Taiwanese and French research vessels, and from several fishing ports located in Japan, Taiwan, and Thailand (Fig. 1). Our analytical results from the multigene phylogenetic inferences and morphometric analyses reveal six putative species within *Lophiomus*, of which three could be aligned to the nominal species (*Lm. setigerus*, *C. malabaricus* and *C. laticeps*) and are discussed hereafter. Three others are new to science and are formally described herein. *Chirolophius laticeps* is resurrected as valid species. However, the taxonomy of *Lp. indicus* and *C. malabaricus* are not treated in this study due to insufficient sampling and information.

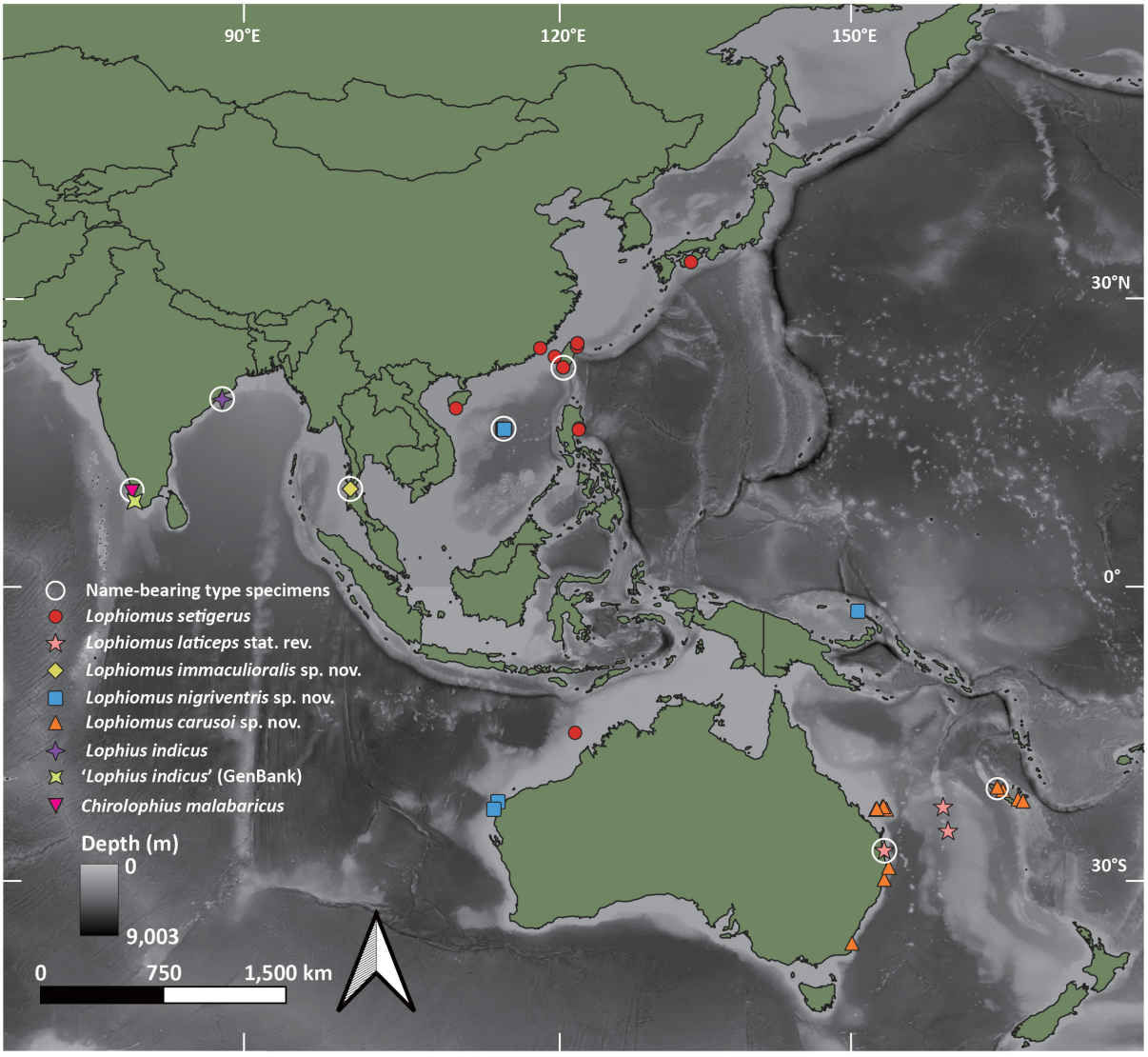

Fig. 1. Bathymetric terrain map of eastern Indian Ocean and West Pacific showing the occurrence points of species of *Lophiomus* Gill, 1883 based on the samples/sequences included in the analyses of this study. White circle: type locality of the species of *Lophiomus*.

Lophiomus setigerus, as well as the genus *Lophiomus*, are redescribed based on data obtained in this study. An identification key to the newly delimited species of *Lophiomus* is provided, and the available diagnostic characters among three morphologically similar genera (*Lophius*, *Lophiomus*, and *Lophiodes*) are also reexamined based on 3D images reconstructed using computed tomography (CT) scanning.

Material and methods

Institutional abbreviations

AMS = Australian Museum, Sydney, Australia
ASIZP = Academia Sinica, Taipei, Taiwan
MNHN = Muséum national d'Histoire naturelle, Paris, France
NHMUK = Natural History Museum, London, United Kingdom
NTUM = National Taiwan University Museums, Taipei, Taiwan

Morphological examination abbreviations

DS2 = The length of the second dorsal-fin spine, measured same as IL
DS3 = The length of the third dorsal-fin spine, measured same as IL
DS4 = The length of the fourth dorsal-fin spine, measured same as IL
HD = Head depth, the distance between the pterotic and lower quadrate spines
HL = Head length, the distance between the premaxillary symphysis and the posteromedial end of the neurocranium
HW = Head width, the distance between the pterotic spines
IF = The distance between the posterior frontal spines
IL = The length of illicium (the first dorsal-fin spine), measured from the base of the spine
ISP = The distance between the inner sphenotic spines
OPSOP = The distance between the left opercular and subopercular spines
PTSP = The distance between the left pterotic and left sphenotic spines
QPAL = The distance between the left lower quadrate and anterior palatine spines
SL = Standard length, in conventional definition
SNL = Snout length, the distance between the premaxillary symphysis and the left posterior frontal spine
SNW = Snout width, the distance between the frontal bones just posterior to their junction with the lateral ethmoids
TL = Tail length, distance between the base of anal-fin and the apex of the caudal fin

Taxon sampling

In the present study, 20 of the 42 specimens of *Lophiomus* were collected from six oceanographic expeditions under the TDSB and TFDeepEvo programs (AURORA 2007, EXBODI, KAVIENG 2014, ZHONGSHA 2015, KANADEEP, and SPANBIOS), and others were collected from fishing ports in Taiwan (Dashi, Nanfangao, Donggang), Penghu Island (Magong), Hainan Island (Sanya), Japan (Mimase, Saga), and Thailand (Ranong) (Fig. 1). Detailed information on the expeditions can be referenced at https://expeditions.mnhn.fr/.

After collection, a small piece of muscle or fin was excised from each sample and preserved in 95% EtOH for DNA analyses. Fresh specimens were then photographed, fixed with 10% formalin, and transferred to 75% EtOH for long-term preservation. Examined specimens were deposited in the ichthyological collections of NTUM and ASIZP.

In addition to the new materials, seven museum voucher specimens of *Lm. setigerus*, and three accessible type specimens of previously described nominal species of *Lophiomus* are also examined and compared (see taxonomy section and Acknowledgements).

Morphological examination and analyses

Morphometric and meristic counting methods, and terminology and abbreviations, follow Caruso (1981, 1983) and were listed above. All specimens were radiographed, and pigmentation was described based on freshly collected specimens with supplemental infromation from preserved specimens (formalin fixation, then transferred to 75% ethanol). The original description of all previously described nominal species of *Lophiomus* were summarized in Table 1. Morphometric measurements of preserved specimens were examined to the nearest 0.1 mm with dial calipers. Measurements of the type specimens (*Lp. indicus* and *C. laticeps*) were carried out from the photos and radiographs of the specimens using sofware ImageJ ver. 1.54f (Schindelin *et al.* 2012). Morphometric measurements are expressed either in percent of standard length (SL) or head length (HL).

Principal component analysis (PCA), Canonical variate analysis (CVA), and biplots of first and second principal components (PC1 and PC2) and canonical variates (CV1 and CV2) of 16 variates (including HL, TL, IL, DS2 and DS3 expressed in percent of the SL; HW, HD, SNL, SNW, ISP, IF, PTSP, QPAL and OPSOP expressed in percent of the HL; and the left pectoral- and pelvic-fin ray counts) from all examined adult *Lophiomus* specimens were conducted in R ver. 4.2.1 (R Core Team 2022). Small specimens (SL < 70 mm), which could be considered as subadults, were excluded from the analyses due to the frequent occurrence of outlier measurements. Missing data estimation were not performed, therefore samples with any missing data were excluded from the analyses.

Computer tomography scanning

The osteological characters of *Lophiomus setigerus*, two of presently described species of *Lophiomus*, and species from other two morphologically similar genera, *Lp. litulon* and *Ld. mutilus*, were examined via computer tomography (CT) scanning (Supp. file 1). Each scan was performed on a whole fixed specimen using a Philips Ingenuity 128 CT scanner (Philips, Amsterdam, Netherlands) at the Taiwan Instrument Research Institute (TIRI), Biomedical Park, Hsinchu, Taiwan. Scanning parameters were as follows, with the surview condition presented in parentheses where they differ: 43 s (4 s) scan time; 80 keV (120 keV) source voltage; 100 mAs (30 mAs) source current; 0.67 mm thickness; 1.4 slice pitch; and 500.00 mm detector to sample distance.

DICOM image stacks were imported into 3DSlicer ver. 5.0.3 (Kikinis *et al.* 2014) to segment the osteological structure by 'threshold' function. Noise and non-target structure (e.g., gut contents) were removed by 'scissors' and 'remove small islands' functions. The surface mesh of each specimen including the entire osteological structure was created in 3Dslicer as an .stl file and then edited in Blender ver. 3.4.1 (Blender Foundation Community 2018).

Molecular data

The total genomic DNA was extracted from tissue samples with commercial DNA extraction kits and automatic extractors: LabTurbo 48 Compact System with LGD 480–500 kits (Taigene Biosciences Corp., Taipei, Taiwan) and QIAcube Connect with Dneasy Blood and Tissue Kit (Qiagen, Düsseldorf, Germany). Four protein-coding genes, comprising two mitochondrial *cytochrome c oxidase I* (*COI*) and *cytochrome b* (*cytb*) genes and two nuclear genes *rhodopsin* and *Recombination activating gene 1* (*RAG1*), were chosen as genetic markers for species delimitation and phylogenetic reconstruction.

Polymerase chain reactions (PCR) used to amplify targeted DNA fragments by primer pairs and conditions follow Huang (2015) and are provided in Supp. file 2. Each PCR was carried out in a 15 µl volume

Table 1. Comparison of the original description of all previously described nominal species of *Lophiomus* Gill, 1883.

	Lophius setigerus Vahl, 1797	*Lophius viviparus* Bloch & Schneider, 1801	*Lophius indicus* Alock, 1889	*Lophiomus longicephalus* Tanaka, 1918	*Chirolophius laticeps* Ogilby, 1910	*Chirolophius malabaricus* Samuel, 1963
Type locality	China	Not described	8 km (5 miles) south of Ganjam, India	Kiinokuni, Tanabe, Japan (current Tanabe-shi, Wakayama Prefecture, Japan)	58 km northeast of Cape Moreton, Queensland, Australia 27°10′ S, 153°17′ E	Kerala coast, southwest India
Depth	Not provided	Not provided	51.2 m (28 fathoms)	Not provided	133.5 m (73 fathoms)	182.8 m (100 fathoms)
Body color	Not described	Not described	Dark gray	Not described	"Pale lilaceous brown"	Brown
Peritoneum color	Not described	Not described	Pale	Not described	White	Pale
Floor of mouth pattern	Black mouth with white spots	Black mouth with white spots	Not described	Black with large white spots, forming black reticulated pattern	"…with blackish anastomosing lines"	Not described
Dorsal-fin spines	4?	Not described	6	6	6	6
Dorsal-fin rays	5	5	8	9	9	9
Anal-fin rays	5	5	6–7	7	7	7
Pectoral-fin rays	10 "…*decem-radiatae*"	Not described	23	Not described	23	24
Pelvic-fin rays	Not described	5	5	Not described	7	5

reagent containing 5.4 µl sterile distilled water, 0.3 µl of each primer (10 µM), 7.5 µl of EmeraldAmp MAX HS PCR Master Mix (Takara Bio., USA), and 1.5 µl of DNA template. Successfully amplified PCR products were then purified by AMPure XP (Beckman Coulter Life Sciences, USA) following the manufacturer's protocol. Sanger sequencing was conducted at Genomics BioSci and Tech (Taipei, Taiwan) with the same primers used for PCR, both strands of the primers being used for sequencing except the *COI* gene, which used the reverse strand only. The obtained sequences were viewed and edited by CodonCode Aligner ver. 10.0.2 (CodonCode Corporation, Dedham, MA, USA).

Automatic multiple sequence alignments were conducted in MAFFT ver. 7 (Katoh *et al.* 2019) with default parameters but choosing 'Adjust direction according to the first sequence' for all four markers. Aligned sequences were then double-checked by translating to amino acids to prevent pseudogene applications using MEGA11 (Tamura *et al.* 2021). If a stop codon occurred, it was considered a pseudogene and excluded from downstream analyses.

Phylogenetic reconstruction

Phylogenetic reconstruction was conducted based on three gene datasets: concatenated mitochondrial (MT; *COI*+*cytb*), concatenated nuclear (NU; *RAG1*+*rhodopsin*), and total-combined (TC; concatenated *COI*+*cytb*+*RAG1*+*rhodopsin*). Only samples with at least one mitochondrial and one nuclear sequence were included in the NU and TC datasets. An additional 31 homologous sequences beyond our four gene markers from 26 samples of *Lophiomus* and one of *Lophius* were retrieved from online databases GenBank (NCBI, Nation Center for Biotechnology Information) (n = 14) and BOLD systems (Ratnasingham & Hebert 2007) (available at: http://v3.boldsystems.org/) (n = 17). Two species of *Lophius*, *Lp. litulon* and *Lp. piscatorius* (Linnaeus, 1758), and one species of *Lophiodes*, *Ld. mutilus*, were sampled as an outgroup for the present phylogenetic reconstruction (Caruso 1985; Miya *et al.* 2010; Carnevale & Pietsch 2012) (Supp. file 1).

Each of the datasets were partitioned first by gene. We then used ModelFinder (Kalyaanamoorthy *et al.* 2017) with the setting 'partition merging' for searching for the best-fit substitution model and partitioning scheme under the corrected Akaike information criterion (AICc). The maximum likelihood method (ML) for all three datasets, and Bayesian Inference (BI) for the TC dataset, were used for phylogenetic reconstruction in the program IQ-TREE ver. 2.1.2 (Minh *et al.* 2020) (ML) and MrBayes ver. 3.2.7a (Ronquist *et al.* 2012) (BI). Nodal support was assessed with ultrafast bootstrap approximation (UFBoot) (Minh *et al.* 2013; Hoang *et al*. 2017) and SH-like approximate likelihood ratio testing (SH-aLRT) (Guindon *et al.* 2010) based on default parameter settings in the ML method and posterior probability (pp.) in the BI method. Nodes with values of SH-aLRT > 80% and UFBoot > 95% were considered as strongly supported nodes.

Species delimitation

The primary species hypotheses (PSHs) for species delimitation were generated based on the supported operational taxonomic units (OTUs) from the monophyly of the MT tree and two DNA-based species delimitation methods: Assemble Species by Automatic Partitioning (ASAP) (Puillandre *et al.* 2020) and Bayesian-based Poisson Tree Processes (bPTP) (Zhang *et al.* 2013). ASAP was conducted separately with *COI* and *cytb* datasets under the K2P distance, and bPTP was conducted separately based on unrooted ML *COI* and *cytb* gene trees. The analyses were performed at web interfaces (ASAP: https://bioinfo.mnhn.fr/abi/public/asap/ and bPTP: https://species.h-its.org/) with default parameter settings. Corrected pairwise genetic distances based on Kimura's two-parameter model (K2P distances) were calculated using MEGA11 to evaluate the degree of interspecific genetic diversity.

The validity of the PSHs were then evaluated by additional criteria, including pairwise genetic distances of the taxa, monophyly found in MT and NU trees, water depth, geographical distribution, and

Table 2. Summarized details for each aligned molecular dataset, including average length of unaligned sequences, length of the aligned dataset, number of variable and parsimony-informative sites, and GC content. Abbreviations: MT = concatenated *COI*+*cytb* dataset; NU = concatenated *RAG1*+*rhodopsin* dataset; Pars-Inf = parsimony-informative sites; TC = concatenated MT+NU dataset.

	Number of sequences	Average length	Aligned length	Variable sites	Pars-Inf sites	GC (%)
COI	44	627.0	663	233	202	49.3
cytb	24	1119.1	1143	460	365	48.0
MT	48	1134.4	1806	693	568	48.7
rhodopsin	18	826.9	900	99	69	54.9
RAG1	15	1436.5	1440	148	83	50.7
NU	18	2023.9	2340	247	152	52.4
TC	18	3653.4	4146	926	696	50.6

morphological comparisons. As suggested by Kekkonen & Hebert (2014) and applied by Hung *et al.* (2017), Lo *et al*. (2017), and Lee *et al.* (2019), sister OTUs from species delimitation analyses were considered as single OTUs rather than multiple OTUs when no other evidence suggested reproductive isolation.

Results

Sequence data

The MT dataset comprises a total of 44 newly obtained sequences (including 20 *COI*, 19 *cytb*, and one *COI*-like pseudogene sequences from *Lophiomus*, and four sequences of both mitochondrial markers from two outgroups, *Lp. litulon* and *Ld. mutilus*), plus 29 available sequences from online databases (including 21 *COI*, two *cytb*, and four *COI*-like pseudogene sequences from *Lophiomus*, and two sequences of both mitochondrial markers from the outgroup *Lp. piscatorius*) (Supp. file 1). In the aligned *COI* dataset, four sequences of *Lophiomus* from Hainan obtained from the BOLD systems (sequence ID: CFCS006-08, CFCS007-08, CFCS138-08, and CFCS139-08) and one *Lophiomus* from Taiwan (sample ID: WJC0905) were found to contain stop codons when translated to amino acids (Supp. file 3). Those sequences were excluded from downstream analyses. Changing the *COI* primer set to FishF2–FishR2 (Ward *et al.* 2005) for the amplification of sample WJC0905 resulted in this resequencing becoming 'normal' (i.e., without a stop codon), so we included this new sequence in the analyzed dataset. The NU dataset comprised a total of 31 newly obtained sequences (including 15 *rhodopsin*, 12 *RAG1* sequences from *Lophiomus*, and four sequences of both nuclear markers from two outgroups, *Lp. litulon* and *Ld. mutilus*), plus two sequences of both nuclear markers from outgroup *Lp. piscatorius* obtained from GenBank (Supp. file 1). No stop codons were found in the aligned NU sequence data. Table 2 summarizes basic information of each aligned gene dataset, including the average length of unaligned sequences, length of aligned sequences, number of variable and parsimony-informative sites, and GC content.

Molecular phylogeny

Figs 2 and 3 show the phylogenetic trees of *Lophiomus* reconstructed by the maximum-likelihood method based on MT and NU datasets, respectively. The monophyly of *Lophiomus* is strongly supported (SH-aLRT/UFBoot = 100/100) in both trees. The MT tree resolves a total of seven independent lineages:

'*Lm*. *setigerus*' from the eastern coast of Australia, *Lm*. 'EAU' from New Caledonia, *Lm. setigerus* from Japan, Taiwan, the South China Sea, and the Timor Sea, '*Lp. indicus*' from southwestern coast of India (K.K. Bineesh personal communication), *Lm*. sp.1 from the South China Sea, Bismarck Sea and western coast of Australia, *Lm*. sp.2 from the Coral Sea, and *Lm*. sp.3 from the Andaman Sea (Figs 1–2). The monophyly of most lineages are highly supported (SH-aLRT > 80% and UFBoot > 95%), the exceptions being *Lm. setigerus* (SH-aLRT / UFBoot = 94.6/87) and the eastern Australian '*Lm*. *setigerus*' (SH-aLRT / UFBoot = 79.3/85), which are only moderately supported. Samples of the eastern Australian '*Lm*. *setigerus*' and '*Lp. indicus*' are not included in the NU tree due to a lack of nuclear gene sequence sampling. Therefore, four resolved lineages or clades (*Lm*. sp.1 + *Lm*. 'EAU', *Lm*. sp.2, *Lm*. sp.3, and *Lm. setigerus*) are illustrated and discussed below.

For intrageneric relationships, the species-level phylogeny of *Lophiomus* reconstructed by the TC dataset is resolved as ((*Lm*. sp. 1, *Lm*. 'EAU'), (*Lm*. sp. 2, (*Lm. setigerus*, *Lm*. sp. 3))) (Fig. 4). The inferred lineages are strongly supported (with SH-aLRT test > 80%, UFBoot > 95%, and pp. > 0.95) except for

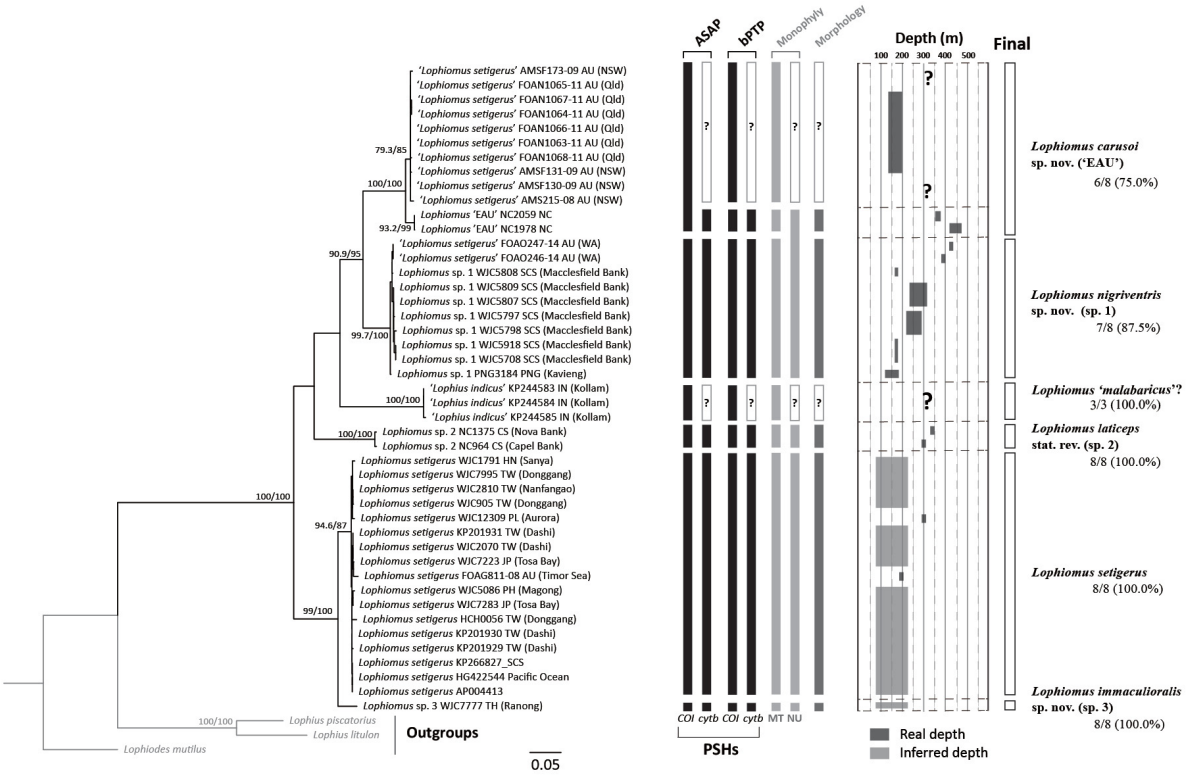

Fig. 2. Maximum-likelihood phylogenetic tree of the species of *Lophiomus* Gill, 1883 based on the MT dataset (1806 bp, *COI*: 663 bp; *cytb*: 1143 bp; TN + F + I (1–663 bp), GTR + F + I + G4 (664–1806 bp)) with species delimitation analyses (vertical bars on the right side of the tree). Branch lengths of the phylogenetic tree are proportional to the inferred nucleotide substitutions except for the one connecting to the distant outgroup of *Lophiodes mutilus*. Node numbers represent 'SH-aLRT / UFBoot' values in percent (%). Locality abbreviations: AU = Australia (NSW = New South Wales; Qld = Queensland; WA = Western Australia); CS = Coral Sea; HN = Hainan Island; IN = India; NC = New Caledonia; PH = Penghu Island; PL = Philippine; PNG = Papua New Guinea; SCS = South China Sea; TH = Thailand; TW = Taiwan. Text next to final decisions represents inferred taxon names and numbers of supported criteria covering all available criteria, with proportions in parentheses.

Lm. setigerus with UFBoot < 95%. The following sister relationships are also strongly supported: between *Lm*. sp. 1 and *Lm*. 'EAU', between *Lm. setigerus* and *Lm*. sp. 3, and between *Lm*. sp. 2 and (*Lm. setigerus*, *Lm*. sp. 3) (Fig. 4).

Principal component analysis and canonical variant analysis

Morphometric measurements are reported in Tables 3–4 and meristic counts in Tables 5–6. Morphometric measurements and meristic counts of *Lophiomus* form four clusters in the PCA biplot: *Lm*. sp. 1, *Lm*. sp. 2, *Lm*. 'EAU', and *Lm. setigerus* (Fig. 5). The 0.68 confidence ellipse of *Lm*. sp. 1 mostly overlaps with that of *Lm. setigerus* (Fig. 5). The sample of *Lm*. sp. 3 is not clustered within any species (Fig. 5). The higher scores of the first principal component (PC1: 35.2% explained variation) suggests higher percentages of OPSOP, QPAL, HW, IF, ISP, SNL, PTSP, HD, and SNW in HL, which contributes to the separation of the *Lm*. 'EAU' cluster from other species. In contrast, the percentages of TL and HL in SL negatively affect the PC1. The second principal component (PC2: 14.0% explained

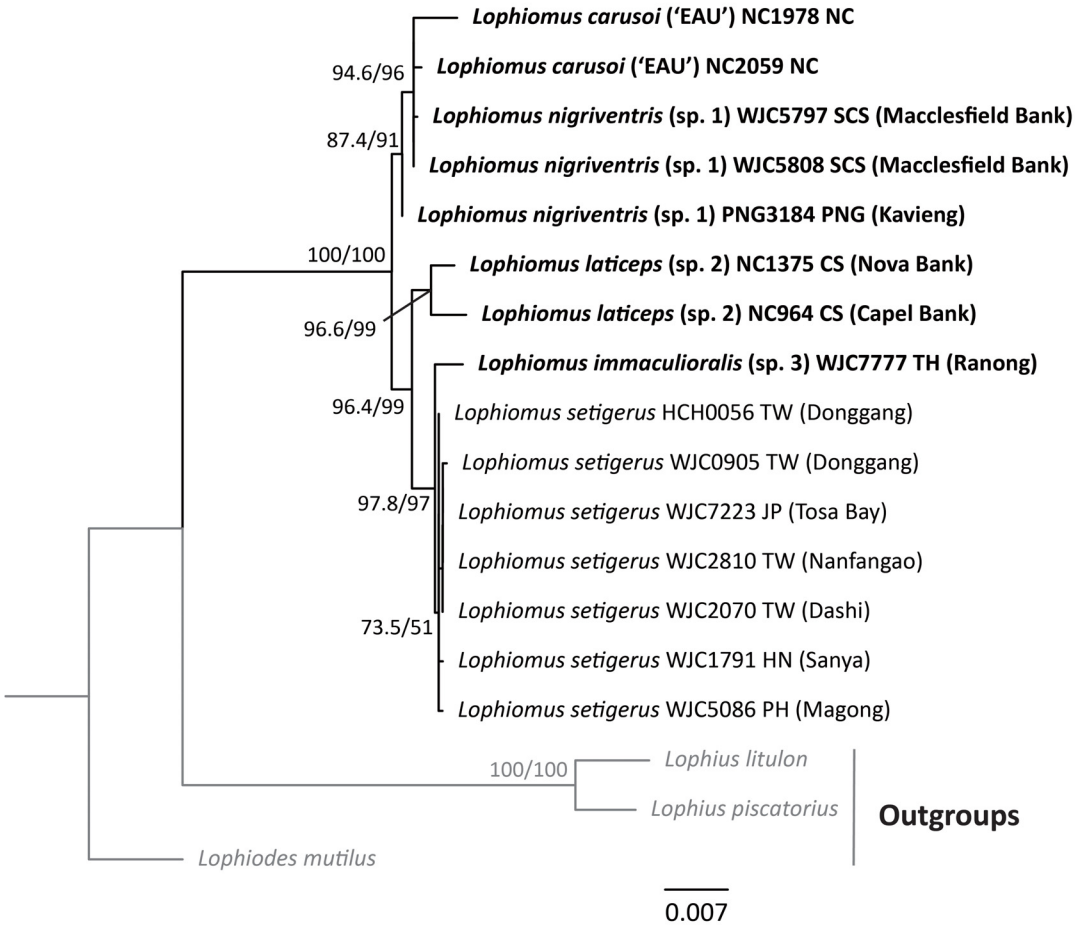

Fig. 3. Maximum-likelihood phylogenetic tree of species of *Lophiomus* Gill, 1883 based on the NU dataset (2340 bp, *RAG1*: 1440 bp; *Rhodopsin*: 900 bp; TPM3u + F + G4 (1–1440 bp), TPM2u + F + I (1441–2340 bp)). Phylogenetic tree branch lengths are proportional to inferred nucleotide substitutions except the connection to distant outgroup *Lophiodes mutilus*. Node numbers represent 'SH-aLRT / UFBoot' values in percent (%). See the caption of Fig. 2 for locality abbreviations. The terminal names in bold suggest the newly described or resurrected taxa in this study.

variation) is positively influenced by the percentages of IL, DS2 and DS3 in SL, and both counts of pectoral-fin and pelvic-fin rays. The equations for PC1 and PC2 are shown in Supp. file 4. The principal component analysis also shows that over 90% of the variance in morphometrics and meristic counts can be summarized within PC1 through PC9.

Each cluster in the CVA result is better separated by the second canonical variant (CV2), although there is overlap between *Lm*. 'EAU', *Lm*. sp. 1, and *Lm*. sp. 2 (Fig. 6). The Linear Discriminant Analysis generating the CVA shows that the first linear discriminant (LD1) is primarily positively influenced by the percentages of IL and DS3 in SL, and SNL in HL, while the second linear discriminant (LD2) is mainly negatively influenced by the percentages of HL, TL, and DS2 in SL, and HD in HL. The equations for LD1 and LD2 are shown in Supp. file 4. The variants that primarily contribute to PC1 and LD2 suggest that they may be potential diagnostic characters for species of *Lophiomus*.

Species delimitation

The *COI*-based ASAP suggests six OTUs within the genus *Lophiomus*, which is mostly congruent with the MT tree except for clustering the eastern Australian '*Lm. setigerus*' and New Caledonian *Lm*. 'EAU' into a single OTU (Fig. 2). In contrast, the *COI*-based bPTP separates the eastern Australian '*Lm. setigerus*' OTU from the New Caledonian *Lm*. 'EAU' OTU, congruent with the MT tree (Fig. 2). Other PSHs (*cytb*-based APSP and bPTP) lacking any sampling of eastern Australian '*Lm. setigerus*' and '*Lp. indicus*' are resolved into only five OTUs (Fig. 2). The *Lm*. sp. 1 and *Lm*. 'EAU' is resolved into multiple OTUs in the MT datasets, whereas all other PSHs are partially congruent with the NU tree (Fig. 3).

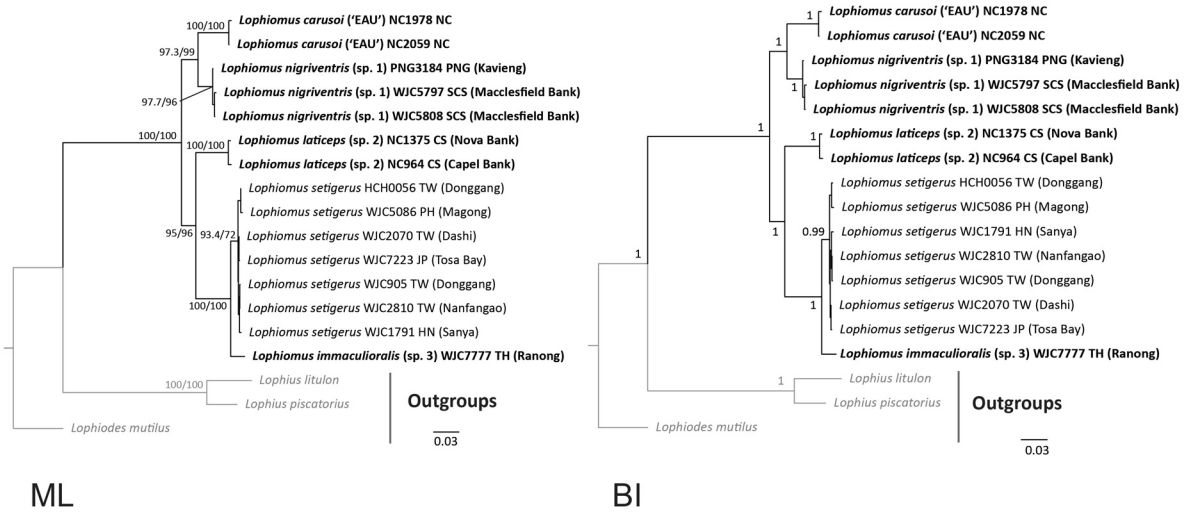

Fig. 4. Phylogenetic trees of species of *Lophiomus* Gill, 1883 reconstructed by partitioned maximum-likelihood and Bayesian inference methods based on the TC dataset (4146 bp, *COI*: 663 bp; *cytb*: 1143 bp; *RAG1*: 1440 bp; *Rhodopsin*: 900 bp; ML: TN+F+I (partition 1, 1–663), GTR+F+I+G4 (partition 2, 664–1806), TPM3+F+G4 (partition 3, 1807–3246), TPM2u+F+I (partition 4, 3247–4146); BI: with the same partition but changed to HKY+I (partition 1), GTR+I+G (partition 2), GTR+G (partition 3), GTR+I (partition 4)). Phylogenetic tree branch lengths are proportional to inferred nucleotide substitutions except the connection to distant outgroup *Lophiodes mutilus*. Node numbers represent 'SH-aLRT/UFBoot/pp.' values, with the former two values expressed in percent (%). See the caption of Fig. 2 for locality abbreviations. Terminal names in bold suggest the newly described or resurrected taxa in this study.

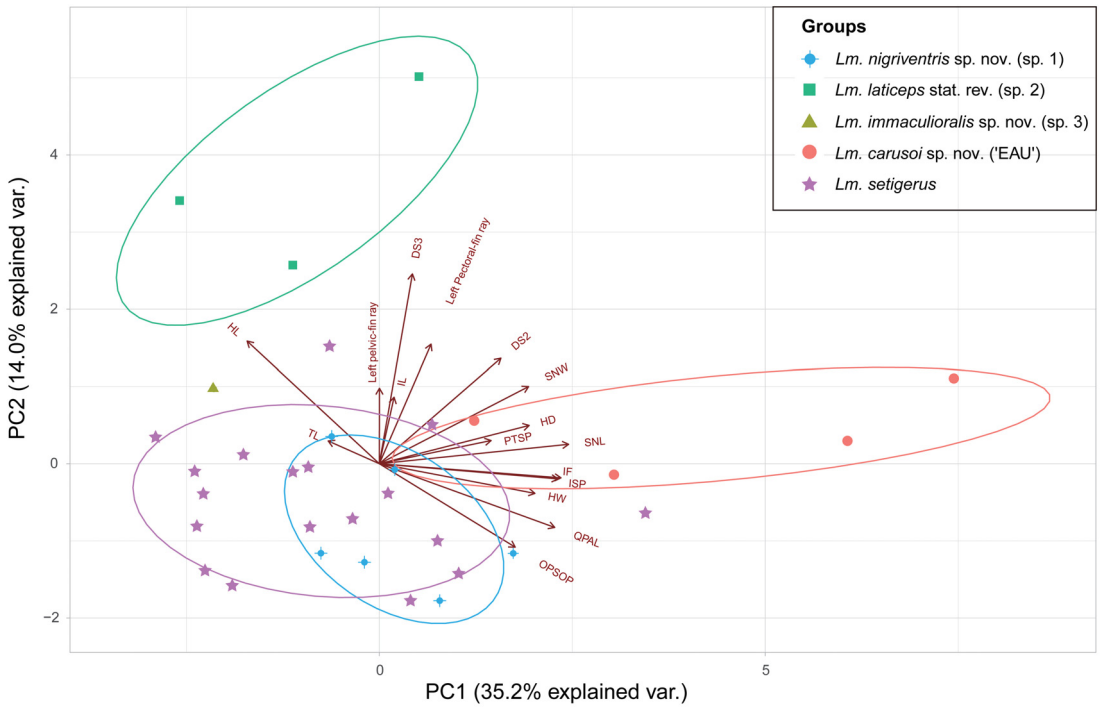

Fig. 5. PCA biplot of the first and second principal components (PC1 and PC2) of species of *Lophiomus* Gill, 1883, with a total of 49.2% of explained variation based on 16 measurements and meristic counts (see Results). Ellipses indicate the confidence interval level set at 0.68 for each group. Arrows represent the direction of the variables projected into the 2D plane of PC1 and PC2.

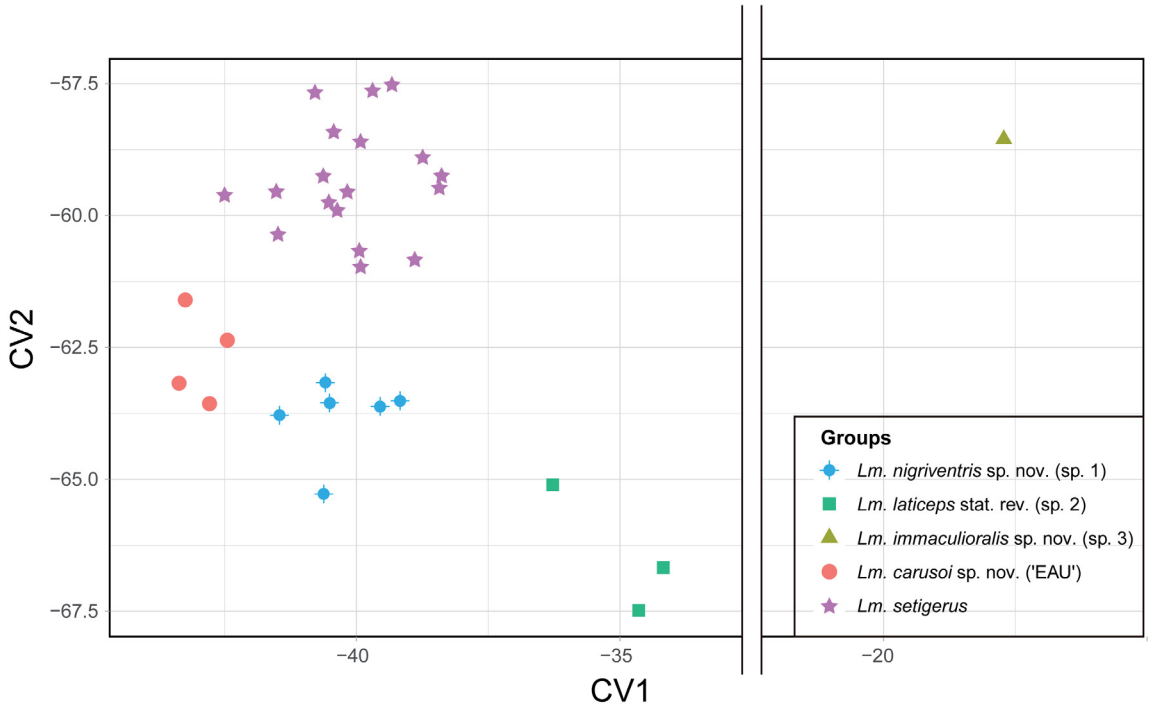

Fig. 6. CVA biplot of the first and second canonical variates (CV1 and CV2) of species of *Lophiomus* Gill, 1883 based on 16 measurements and meristic counts (see Results).

Table 3. Standard length and the measurements expressed in percent (%) of standard length of species of *Lophiomus* Gill, 1883 described in this study. Values are expressed as ranges; values in parentheses are means ± standard deviations. Definitions and measurement abbreviations follow Caruso (1981). Abbreviations: HT = Holotype; N/A = unavailable; NT = neotype; ST = syntypes.

Species	***Lm. laticeps*** stat. rev.		***Lm. nigriventris*** sp. nov.			***Lm. immaculioralis*** sp. nov.	***Lm. carusoi*** sp. nov.		***Lm. setigerus***			***Lp. indicus***
	HT	adults n = 3	**HT**	adults n = 6	subadult n = 1	**HT**	**HT**	adults n = 4	**NT**	this study n = 18	(Caruso 1983) n = 41	**ST** (subadults) n = 2
SL (mm)	145.1	145.1–237.1 (178.3 ± 51.0)	193.2	147.4–220.8 (188.0 ± 23.6)	34.8	243.0	263.5	121.0–292.5 (228.0 ± 75.1)	155.0	69.3–284.3 (174.6 ± 65.8)	70.0–277.0	35.3–66.4
HL	39.9	34.2–39.9 (36.2 ± 0.03)	31.7	28.8–33.3 (30.9 ± 0.02)	24.1	31.9	32.7	28.4–32.7 (29.8 ± 0.02)	28.8	27.3–36.7 (32.1 ± 0.02)	32.1–40.2	40.7–41.9
TL	56.5	45.4–56.5 (50.2 ± 0.06)	50.3	47.0–50.3 (49.0 ± 0.01)	49.4	46.0	51.5	47.4–51.5 (48.8 ± 0.02)	48.3	38.6–55.4 (49.5 ± 0.05)	31.5–39.0	55.1–56.9
IL	23.3	23.3–31.3 (226.5 ± 0.04)	29.0	16.5–29.0 (23.6 ± 0.04)	23.9	30.7	33.7	24.6–33.7 (27.9 ± 0.04)	23.4	21.4–32.7 (26.2 ± 0.03)	23.3–41.7	20.7–23.9
DS2	17.4	17.4–25.5 (22.0 ± 0.04)	20.7	17.9–20.7 (19.5 ± 0.01)	23.0	18.3	22.0	19.7–23.1 (21.9 ± 0.02)	17.3	15.0–25.7 (18.7 ± 0.03)	13.2–20.8	26.6–27.6
DS3	27.3	27.3–33.7 (31.0 ± 0.03)	21.8	18.9–24.0 (21.2 ± 0.02)	34.5	23.5	19.3	19.3–28.9 (23.8 ± 0.04)	21.2	16.3–25.5 (21.8 ± 0.02)	13.5–25.3	69.2 (n = 1)
DS4	N/A	20.5–26.0 (n = 2)	17.0	8.4–17.3 (14.7 ± 0.04)	26.1	19.7	16.7	16.7–24.0 (19.5 ± 0.03)	18.3	12.0–25.1 (19.0 ± 0.03)	N/A	N/A

Table 4. Measurements expressed in percent (%) of head lengths of species of *Lophiomus* Gill, 1883 described in this study. Values are expressed as ranges; values in parentheses are means ± standard deviations. Definitions and measurement abbreviations follow Caruso (1981). Abbreviations: HT = Holotype; N/A = unavailable; NT = neotype; ST = syntypes.

Species	***Lm. laticeps*** stat. rev.		***Lm. nigriventris*** sp. nov.			***Lm. immaculioralis*** sp. nov.	***Lm. carusoi*** sp. nov.		***Lm. setigerus***			***Lp. indicus***
	HT	adults n = 3	**HT**	adults n = 6	subadult n = 1	**HT**	**HT**	(adults) n = 4	**NT**	(this study) n = 18	(Caruso 1983) n = 41	**ST** (subadults) n = 2
HW	54.1	50.7–54.3 (53.0 ± 0.02)	56.4	52.8–62.0 (57.8 ± 0.03)	81.0	54.9	58.1	58.1–68.6 (63.2 ± 0.04)	51.7	37.4–59.2 (54.5 ± 0.05)	52.2–58.4	57.7–61.5
HD	85.3	69.3–85.3 (76.1 ± 0.08)	74.2	69.4–80.1 (73.8 ± 0.04)	107.1	71.2	77.9	77.9–88.6 (82.0 ± 0.05)	79.6	66.4–82.4 (72.7 ± 0.04)	66.4–74.7	60.3–60.4
SNL	56.6	56.6–66.3 (62.4 ± 0.05)	64.6	54.2–66.2 (62.9 ± 0.04)	114.9	57.9	63.8	63.8–82.9 (71.4 ± 0.08)	65.5	56.0–71.4 (61.4 ± 0.04)	53.1–59.0	54.4–58.5
SNW	39.6	30.9–56.5 (42.3 ± 0.13)	38.3	31.8–39.5 (35.8 ± 0.04)	70.2	37.6	41.9	41.9–55.7 (48.9 ± 0.06)	32.7	28.5–47.9 (38.6 ± 0.06)	20.7–25.1	25.3–36.3
ISP	39.9	39.2–39.9 (39.6 ± 0.003)	41.1	40.6–45.4 (43.1 ± 0.02)	65.5	40.3	53.1	48.6–56.7 (52.3 ± 0.03)	46.1	33.0–49.0 (41.2 ± 0.04)	36.7–44.3	34.2–42.2
IF	32.8	31.9–35.9 (33.5 ± 0.02)	37.2	35.9–37.4 (36.7 ± 0.01)	41.7	32.7	35.3	35.3–55.8 (45.9 ± 0.09)	35.6	30.9–41.1 (35.6 ± 0.03)	31.5–38.4	21.3–31.1
PTSP	16.1	12.3–16.1 (14.3 ± 0.02)	14.4	13.3–16.7 (14.9 ± 0.01)	25.0	14.5	14.2	10.7–19.6 (15.8 ± 0.04)	11.9	10.7–16.4 (13.5 ± 0.01)	11.4–15.2	19.6–22.4
QPAL	51.6	51.6–63.6 (58.8 ± 0.06)	68.7	65.5–74.1 (69.0 ± 0.03)	101.2	64.7	64.0	64.0–82.9 (73.4 ± 0.09)	72.3	47.3–76.2 (65.2 ± 0.07)	62.3–72.0	60.5–70.7
OPSOP	31.6	31.6–47.4 (40.7 ± 0.08)	50.2	47.3–53.6 (49.5 ± 0.02)	58.3	22.2	55.5	55.5–65.7 (59.6 ± 0.04)	57.0	46.1–60.0 (51.9 ± 0.03)	47.8–54.0	35.6–49.3

Table 5. Meristic counts of species of *Lophiomus* Gill, 1883 described in this study. Values are counted from both sides and expressed as ranges; values expressed in parentheses indicate counts from the right side. Abbreviations: HT = Holotype; N/A = unavailable; NT = neotype; ST = syntypes.

Species	***Lm. laticeps*** stat. rev.		***Lm. nigriventris*** sp. nov.		***Lm. immaculioralis*** sp. nov.	***Lm. carusoi*** sp. nov.		***Lm. setigerus*** (this study)		***Lm. setigerus*** (Caruso 1983)	***Lp. indicus***
	HT	adults n = 3	**HT**	adults n = 7	**HT**	**HT**	adults n = 4	**NT**	adults n = 18	n = 41	**ST** n = 2
Dorsal-fin spines	6	6	6	6	5	6	6	6	6	6	6
Dorsal-fin rays	8	8	8	8	8	8	8	8	8	8	8
Anal-fin rays	6	6	6	6	6	6	6	6	6	6	6
Pectoral-fin rays	24 (24)	24–25 (24–25)	23 (24)	23–24 (23–24)	22 (21)	23 (23)	23–24 (23–24)	22 (22)	21–23 (21–23)	21–25	22 (23)
Pelvic-fin rays	7 (7)	7 (7)	6 (6)	6 (6)	7 (7)	7 (7)	7 (7)	7 (7)	6–7 (6–7)	N/A	7 (7)
Vertebrae	18	18–19	18	18	18	18	18	19	18–19	18–19	18
Outermost row of premaxillary teeth	N/A	15–18 (17–22)	22 (21)	17–21 (17–24)	33 (35)	22 (20)	15–27 (12–22)	25 (27)	18–33 (27–33)	6–18	N/A
Interopercular spines	2	2	2	2	2	2	2	2	2	2	2
Branchiostegal rays	5	5	5	5	5	5	5	5	5	N/A	5

Table 6. Frequency distribution of left (upper row) and right (lower row) pectoral-fin rays and vertebrae meristic counts of species of *Lophiomus* Gill, 1883 described in this study. The star mark indicates the count of the name-bearing type. Abbreviations: Mean = arithmetic mean of meristic counts; N = number of examined specimens.

	Pectoral-fin rays								Vertebrae				
	N	Mean	21	22	23	24	25	26	N	Mean	18	19	20
Lm. setigerus	13	22.1	1	10*	2				4	18.25	3	1*	
	13	21.9	2	10*	1								
Lm. laticeps stat. rev.	3	24.3				2*	1		3	18.3	2*	1	
	3	24.3				2*	1						
Lm. nigriventris sp. nov.	7	23.3			5*	2			6	18	6*		
	7	23.3			5	2*							
Lm. carusoi sp. nov.	4	23.3			3*	1			2	18	2*		
	4	23.3			3*	1							
Lm. immaculioralis sp. nov.	1	22		1*					1	18	1*		
	1	21	1*										
Lp. indicus	1	23			1*				2	18	2*		
	2	22		2*									

Table 7. Mean pairwise K2P distances and estimated variance of *COI* and *cytb* sequences of specie of *Lophiomus* Gill, 1883 included in this study. The values in the lower left of the matrix represent the K2P distances, and the upper right represents the variances estimated by the Bootstrap method in 500 replications. Bolding indicates the species newly described in this study. Abbreviations: EAU = Eastern Australia; NC = New Caledonia; N/A = unavailable.

COI

	Lm. setigerus	***Lm. immaculioralis*** sp. nov.	***Lm. laticeps*** stat. rev.	***Lm. carusoi*** sp. nov. **(EAU)**	***Lm. carusoi*** sp. nov. **(NC)**	***Lm. nigriventris*** sp. nov.	'***Lp. indicus***'	Intraspecific mean distance
Lm. setigerus		0.0089	0.0164	0.0197	0.0200	0.0185	0.0190	0.0081
Lm. immaculioralis sp. nov.	0.0513		0.0165	0.0191	0.0194	0.0175	0.0181	N/A
Lm. laticeps stat. rev.	0.1366	0.1405		0.0203	0.0206	0.0171	0.0195	0
Lm. carusoi sp. nov. (EAU)	0.1860	0.1799	0.1781		0.0057	0.0127	0.0171	0.0027
Lm. carusoi sp. nov. (NC)	0.1863	0.1783	0.1800	0.0234		0.0132	0.0175	0.0016
Lm. nigriventris sp. nov.	0.1658	0.1516	0.1469	0.0979	0.1030		0.0170	0.0051
'***Lp. indicus***'	0.1718	0.1609	0.1753	0.1490	0.1518	0.1480		0.0021

cytb

	Lm. nigriventris sp. nov.	***Lm. carusoi*** sp. nov. **(NC)**	***Lm. laticeps*** stat. rev.	***Lm. setigerus***	***Lm. immaculioralis*** sp. nov.	Intraspecific mean distance
Lm. nigriventris sp. nov.		0.0103	0.0143	0.0137	0.0146	0.0053
Lm. carusoi sp. nov. (NC)	0.1092		0.0139	0.0147	0.0154	0
Lm. laticeps stat. rev.	0.1631	0.1785		0.0125	0.0130	0.0079
Lm. setigerus	0.1671	0.1819	0.1594		0.0073	0.0046
Lm. immaculioralis sp. nov.	0.1701	0.1886	0.1658	0.0528		N/A

Measured pairwise K2P distances of *COI* and *cytb* sequences are provided in Table 7. The mean K2P distances of *COI* and *cytb* sequences among different OTUs from PSHs are mostly larger than 0.1; the distance between *Lm. setigerus* and *Lm*. sp. 3 is moderately high at *COI* (0.0513) and at *cytb* (0.0528). However, the distance between eastern Australian '*Lm. setigerus*' and *Lm*. 'EAU' is only 0.0234 at *COI* which is lower than mean value from a sibling pair of marine fishes (Ward 2009; Zemlak *et al*. 2009).

Morphological comparisons show that the inferred OTUs from the PSHs can be separated by a combination of characters such as body color, pattern of the floor of mouth, counts of pectoral-fin rays, pelvic-fin rays, and several measurements of cranial spines. Detailed information for these is provided in the taxonomy section below. Most of the samples from these OTUs were collected from 100 to 300 m depths, but the two western Australian *Lm*. sp. 1, all *Lm*. sp. 2 samples and the two New Caledonian *Lm*. 'EAU' samples were from depths below 300 m.

Combining all species delimitation criteria mentioned above, we suggest six inferred species of which sp. 1, sp. 3, and 'EAU' are described herein as *Lm. nigriventris* sp. nov., *Lm. immaculioralis* sp. nov., and *Lm. carusoi* sp. nov., respectively. By further examining the photos and radiographs of type specimens of *Lp. indicus* and *C. laticeps* together with the original description of all previously described nominal species for *Lophiomus* (Table 1), it is considered that sp. 2 is conspecific to *C. laticeps* based on shared features in body coloration, counts of pectoral- and pelvic-fin rays, and pattern of the floor of mouth. *Lm. setigerus* remains within the same taxonomic status; its redescription is conducted herein based on new samples and information obtained in this study. However, the taxonomy of '*Lp*. *indicus*' requires more evidence for final validation (see Discussion).

Computer tomography scanning

CT-scanning of two species from two morphologically similar genera of *Lophiomus*, *Lp. litulon* and *Ld. mutilus*, were performed to re-examine the generic diagnostic characters proposed by Caruso (1981, 1983). The information of non-*Lophiomus* specimens used for comparison is listed below:

BISMARK SEA • 220.0 mm SL, sample ID: NC1541; West Pacific, Bismark Sea, Papua New Guinea, NW off Aitape, stn CP4055; 03°03′ S, 142°18′ E; 370–374 m deep; 20 Dec. 2012; R/V *ALIS*; French beam trawl; PAPUA NEW GUINI exped.; Voucher: NTUM10390. [Identification: *Lophiodes multilus*.]

NORTHWEST PACIFIC • 370.0 mm SL, sample ID: WJC7228; Japan, Tosa Bay, Mimase fish port; ca 100–200 m deep; 28 Jan. 2018; Voucher: NTUM14415. [Identification: *Lophius litulon*.]

The reconstructed 3D models were output as .stl file and attached in Supp. file 5. The osteological comparison among *Lophiomus*, *Lophius*, and *Lophiodes* by CT-scanning is mostly congruent with the previous descriptions in Caruso (1981, 1983) (Fig. 7). The revised generic definition and diagnosis of genus *Lophiomus* by including newly described species are summarized in Taxonomy section below.

Taxonomy

Class Actinopterygii Klein, 1885
Order Lophiiformes Garman, 1899
Family Lophiidae Rafinesque, 1810

Genus ***Lophiomus*** Gill, 1883

Lophiomus Gill, 1883 [1882]: 552. Type species: *Lophius setigerus* Vahl, 1797. Original designation.

Diagnosis

Lophiomus can be separated from other extant lophiid genera by the combination of vertebrae 18–19; dorsal-fin rays 8; anal-fin rays 6; flat body shape; presence of third dorsal-fin spine, humeral, and subopercular spines; rugose frontal ridge; gill opening not extending anterior to the pectoral-fin base; single articular spine; single quadrate spine; two sphenotic spines; two interopercular spines; the outer surface of maxilla bearing low and conical knobs; ural centrum bearing transverse processes; and the floor of mouth with distinct dark pigmentations (except *Lm. immaculioralis*).

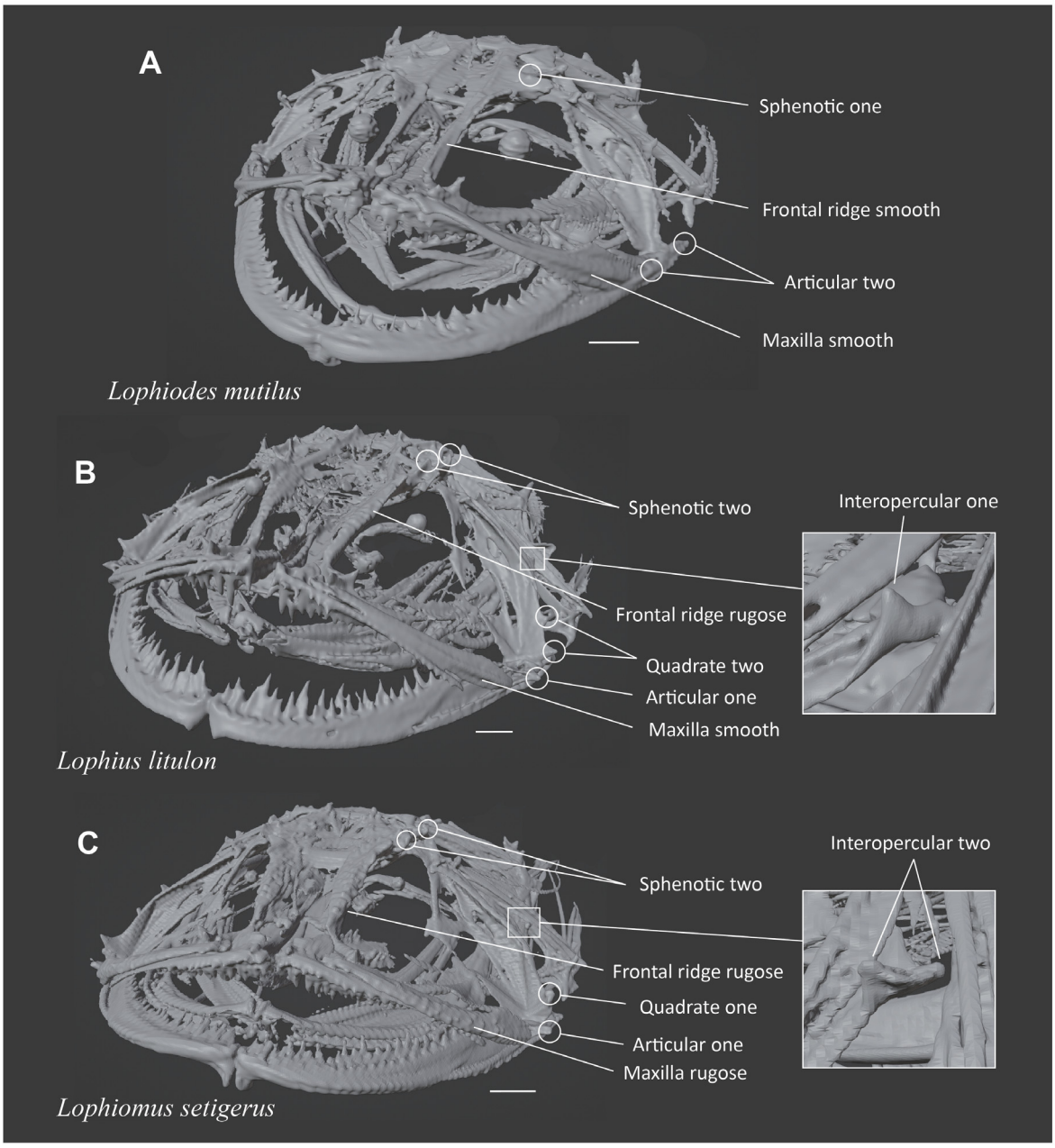

Fig. 7. Cranial comparative osteology of the three lophiid genera. **A**. *Lophiodes mutilus* (Alcock, 1894). **B**. *Lophius litulon* (Jordan, 1902). **C**. *Lophiomus setigerus* (Vahl, 1797). Scale bars = 10 mm.

Differential diagnosis

Lophiomus can be readily distinguished from *Sladenia* by its flat body shape (body shape rounded in *Sladenia*). Among the flat-bodied lophiid genera, *Lophiomus* can be differentiated from *Lophiodes* by its rugose frontal ridge (frontal ridge smooth in *Lophiodes*), gill opening not extending anteriorly to the pectoral-fin base (gill opening extending anterior to the pectoral-fin base in *Lophiodes*), a single articular spine (two articular spines in *Lophiodes*), two sphenotic spines (one inner sphenotic spine in *Lophiodes*), and one ural centrum bearing transverse processes (ural centrum without transverse processes in *Lophiodes*) (Fig. 7, Supp. file 5). *Lophiomus* can also be distinguished from its sibling genus *Lophius* in having vertebrae 18–19 (vertebrae more than 20 in *Lophius*), dorsal-fin rays 8 (9–12 in *Lophius*; Caruso 1985), anal-fin rays 6 (8–10 in *Lophius*; Caruso 1985), interopercular with two spines (single spine in *Lophius*), the outer surface of maxilla bearing low and conical knobs (smooth outer surface in *Lophius*), and quadrate with a single spine (two spines in *Lophius*) (Fig. 7, Supp. file 5).

General description

Measurements and meristic counts. Dorsal-fin spines 5–6; dorsal-fin rays 8; anal-fin rays 6; pectoral-fin rays 21–26; pelvic-fin rays 6–7; branchiostegal rays 5; interopercular spines 2; vertebrae 18–19; outermost row of premaxillary teeth 6–35. SL 69.3–292.5 mm; HL 27.3–39.9%, TL 41.0–59.6%, IL 16.5–33.7%, DS2 15.0–25.7%, DS3 16.3–33.7%, DS4 8.4–26.0% of SL; HW 37.4–68.6%, HD 69.3–88.6%, SNL 54.2–82.9%, SNW 28.5–56.5%, ISP 33.0–56.7%, IF 30.9–55.8%, PTSP 10.7–19.6%, QPAL 47.3–82.9%, OPSOP 31.6–65.7% of HL (adults).

Head and body. Body shape strongly depressed; gill opening not reaching beyond base of pectoral-fin base; pectoral-fin broad; frontal ridge and outer surface of maxilla (and dentary in some species) rugose, bearing low conical knobs; parietal spines strong and sharp; quadrate with single lower spine; inner and outer sphenotic spines well developed; epiotic spines well developed; articular spine one, antero-lateral to jaw joint; subopercular spine one; interopercular spines two; humeral spine well developed and complex, with three to five spinelets; ural centrum depressed, with transverse process; eye suboval; esca pennant-like or tassel-like flap; preserved coloration pale khaki to brown dorsally; light ventrally; peritoneum pigmentation from light to dark; floor of mouth with dark pigmentations except *Lm. immaculioralis* sp. nov., ranging from light background with reticulate dark pattern, anastomosing dark pattern, to dark background with circular or irregular pale pattern; lateral surface of lower jaw, head, and caudal peduncle with well-developed tendrils.

Remarks

This genus was thought to be monotypic since Caruso (1983). The present study re-defines it by including the result of CT-scan and the descriptions of four additional species. Unlike the characteristics described by Caruso (1983, 1985) for this genus, which include a floor of the mouth with a distinct dark marking and 6 dorsal-fin spines, the newly described species, *Lm. immaculioralis* sp. nov., features a floor of the mouth without a distinct dark marking and 5 dorsal-fin spines. Consequently, the generic definition of this genus is herein revised accordingly.

It is noteworthy that meristic counts of dorsal-fin rays and anal-fin rays were often misinterpreted in studies conducted before Caruso (1983) when X-ray or CT scanning was not available for the examinations (Table 1). The dorsal-fin rays are found to be forked in the last ray at least in *Lm. laticeps* (Fig. 10E), which may have led previous researchers to miscount the dorsal-fin rays as nine. The anal-fin rays were also miscounted as seven in previous descriptions (Table 1).

Lophiomus setigerus (Vahl, 1797)
urn:lsid:zoobank.org:act:2AD07693-B224-4DCE-ADC3-267902D186ED
Figs 7C, 8–9, 15A, 16G–H; Tables 1, 3–6

Lophius setigerus Vahl, 1797: 215.
Lophius viviparus Bloch & Schneider, 1801: 142. Objective synonym.
Lophius indicus Alcock, 1889: 302. Synonymized by Caruso 1983: 13.
Lophiomus longicephalus Tanaka, 1918: 227. Synonymized by Caruso 1983: 13.

Diagnosis

This species can be separated from other congeners by the combination of dorsal-fin spines 6, pelvic-fin rays mostly 7, pectoral-fin rays 21–23 (mostly 22; Table 6), brown body coloration, peritoneum with gray pigmentation, and circular or irregular light pattern on the dark floor of the mouth.

Pseudogene was detected from the DNA barcode region (COI-5P) of *COI* gene in real *Lm. setigerus* by primer pair FishF1–FishR1 (Ward *et al.* 2005) and cocktail primers C_VF1LFt1–C_VR1LRt (Ivanova *et al.* 2007), with stop codon occurring at amino acid position 27 in sample WJC0905 (nucleotide position 79–81 'AGG', but 'GGA' normally), and position 79 in samples WJC0905, CFCS006-08, CFCS007-08, CFCS138-08, and CFCS139-08 (nucleotide position 235–237 'AGG', but 'GGG' or 'GGC' normally) in the *COI* dataset in this study (Supp. file 3). Numbering of the position starts from the first amino acid or nucleotide site of the gene.

Differential diagnosis

Lophiomus setigerus is most similar to its sibling species *Lm. immaculioralis* sp. nov. in the brown body coloration and pectoral-fin ray counts. However, it differs by having a higher count of dorsal-fin spines (6 vs 5 in *Lm. immaculioralis*), an esca that is mostly pennant-like (tassel-like flap in *Lm. immaculioralis*), peritoneum with gray pigmentation (lacking dark or gray pigmentation in *Lm. immaculioralis*), and a dark floor of the mouth with circular or irregular light patterns (absence of distinct dark markings in *Lm. immaculioralis*). The molecular diagnosis is elaborated in the differential diagnosis section of *Lm. immaculioralis*.

This species also shares similarities with the newly described species *Lm. carusoi* sp. nov. in the brown body coloration but differs in having lower counts of dorsal-fin spines (21–23, mostly 22 vs 23–24 in *Lm. carusoi*; Table 6), a narrower HW (37.4–59.2% HL vs 58.1–68.6% HL in *Lm. carusoi* sp. nov.; Table 4), a narrower ISP (33.0–49.0% HL vs 48.6–56.7% HL in *Lm. carusoi*; Table 4), and a dark floor of the mouth with circular or irregular light patterns (a light floor of the mouth with a reticulate dark pattern in *Lm. carusoi*).

Furthermore, this species can be distinguished from the potentially sympatric newly described species, *Lm. nigriventris* sp. nov., by its brown body coloration (pale khaki of *Lm. nigriventris*), gray peritoneum (dark in *Lm. nigriventris*), and a dark floor of the mouth with circular or irregular light patterns (light floor of the mouth with reticulate dark pattern in *Lm. nigriventris*).

Material examined

Neotype (designated here)
TAIWAN STRAIT • 155.0 mm SL, sample ID: WJC0905; Taiwan, Pingtung County, Donggang fish port; ca 100–200 m deep; 13 Apr. 2012; GenBank nos: OR262148 (*COI*), OR257544 (*cytb*), OR260582 (*rhodopsin*), OR257559 (*RAG1*), OR260592 (*COI*-like pseudogene); Voucher: NTUM10408.

Non-type material

NORTHWEST PACIFIC • 284.3 mm SL, sample ID: WJC7223; Japan, Tosa Bay, Mimase fish port; ca 100–200 m deep; 28 Jan. 2018; GenBank nos: OR262050 (*COI*), OR257546 (*cytb*), OR260589 (*rhodopsin*), OR257560 (*RAG1*); Voucher: NTUM14414 • 271.1 mm SL, sample ID: WJC7224; same data as for preceding; Voucher: NTUM14414 • 194.3 mm SL, sample ID: WJC7225; same data as for preceding; Voucher: NTUM14414 • 210.8 mm SL, sample ID: WJC7226; same data as for preceding; Voucher: NTUM14414 • 198.1 mm SL, sample ID: WJC7226; same data as for preceding; Voucher: NTUM14414 • 81.9 mm SL, sample ID: WJC7283; Japan, Tosa Bay, Saga fish port; ca 100–200 m deep; 31 Jan. 2018; GenBank nos: OR262051 (*COI*), OR257551 (*cytb*); Voucher: NTUM14414.

PHILIPPINE SEA • 77.0 mm SL; Philippines, Aurora, stn CP2653; 121°59′45″ E, 16°06′30″ N; 82.7 ± 50 m deep; 20 May 2007; Voucher: ASIZP67752 • 99.0 mm SL; same data as for preceding, stn CP2654; 121°57′30″ E, 16°04′44″ N; 98.4–107 m deep; 20 May 2007; Voucher: ASIZP67786.

SOUTH CHINA SEA • 107.0 mm SL, sample ID: WJC1791; China, Hainan, Sanya fish port; ca 100–200 m deep; 27 Jul. 2010; GenBank nos: OR257545 (*cytb*), OR260585 (*rhodopsin*), OR257561 (*RAG1*); Voucher: NTUM10413.

TAIWAN STRAIT • 69.3 mm SL, sample ID: WJC7008; Taiwan, Pingtung County, Donggang fish port; ca 100–200 m deep; 27 Feb. 2017; Voucher: NTUM15739 • 264.1 mm SL, sample ID: WJC5086; Taiwan, Penghu Island, Magong third fish port; ca 100–200 m deep; 3 May 2015; GenBank nos: OR257549 (*cytb*), OR260580 (*rhodopsin*), OR257558 (*RAG1*); Voucher: NTUM14640.

WEST PACIFIC • 180.0 mm SL, sample ID: WJC2070; Taiwan, Yilan County, Dashi fish port; 121°54′03″ E, 24°56′27″ N; ca 100–200 m deep; 9 Apr. 2013; GenBank nos: OR262149 (*COI*), OR257548 (*cytb*), OR260583 (*rhodopsin*); Voucher: NTUM10414 • 204.0 mm SL, sample ID: WJC5434; same data as for preceding; 16 Jun. 2015; Voucher: NTUM16309 • 198.0 mm SL, sample ID: WJC8060; same data as for preceding; 14 Apr. 2018; Voucher: NTUM15875 • 190.0 mm SL; same data as for preceding; 27 Feb. 2003; GenBank no.: KP201930 (*COI*); Voucher: ASIZP62543 • 193.0 mm SL; same data as for preceding; GenBank no.: KP201929 (*COI*); Voucher: ASIZP62544 • 165.0 mm SL; same data as for preceding; GenBank no.: KP201931 (*COI*); Voucher: ASIZP62545.

Comparative material

Syntypes of *Lophius indicus* Alock, 1889

INDIAN OCEAN • 66.4 mm SL; India, Bay of Bengal, 8 km (5 miles) south of Ganjam; ca 51 m (28 fathoms) deep; Voucher: BMNH 1890.11.28.45 • 35.3 mm SL; same data as for preceding; BMNH 1890.11.28.46.

Redescription of adults

Measurements and meristic counts. Morphometric values given in Tables 3 and 4. Dorsal-fin spines 6; dorsal-fin rays 8; anal-fin rays 6; pectoral-fin rays 21–23; pelvic-fin rays 6–7; branchiostegal rays 5; quadrate spine 1; interopercular spines 2; vertebrae 18–19; outermost row of premaxillary teeth 17–24 (Tables 5–6).

Head and body. Head length short to moderately long (27.3%–36.7% of SL, mean 32.1 ± 0.02%); head width relatively narrow to moderately wide (37.4%–59.2% of HL (mean 54.5 ± 0.05%); eyes suboval; anterior half of premaxilla with three rows of enlarged teeth, largest on innermost row, followed by single row of small teeth on posterior half; maxilla toothless; palatine with single row of small teeth, with some enlarged; dentary with three rows of teeth, outer teeth minute and innermost teeth largest; fifth ceratobranchial with two rows of small teeth, forming V-shaped patch; teeth on second and third pharyngobranchials forming small and rounded patches; gill rakers and pseudobranch absent. Palatine

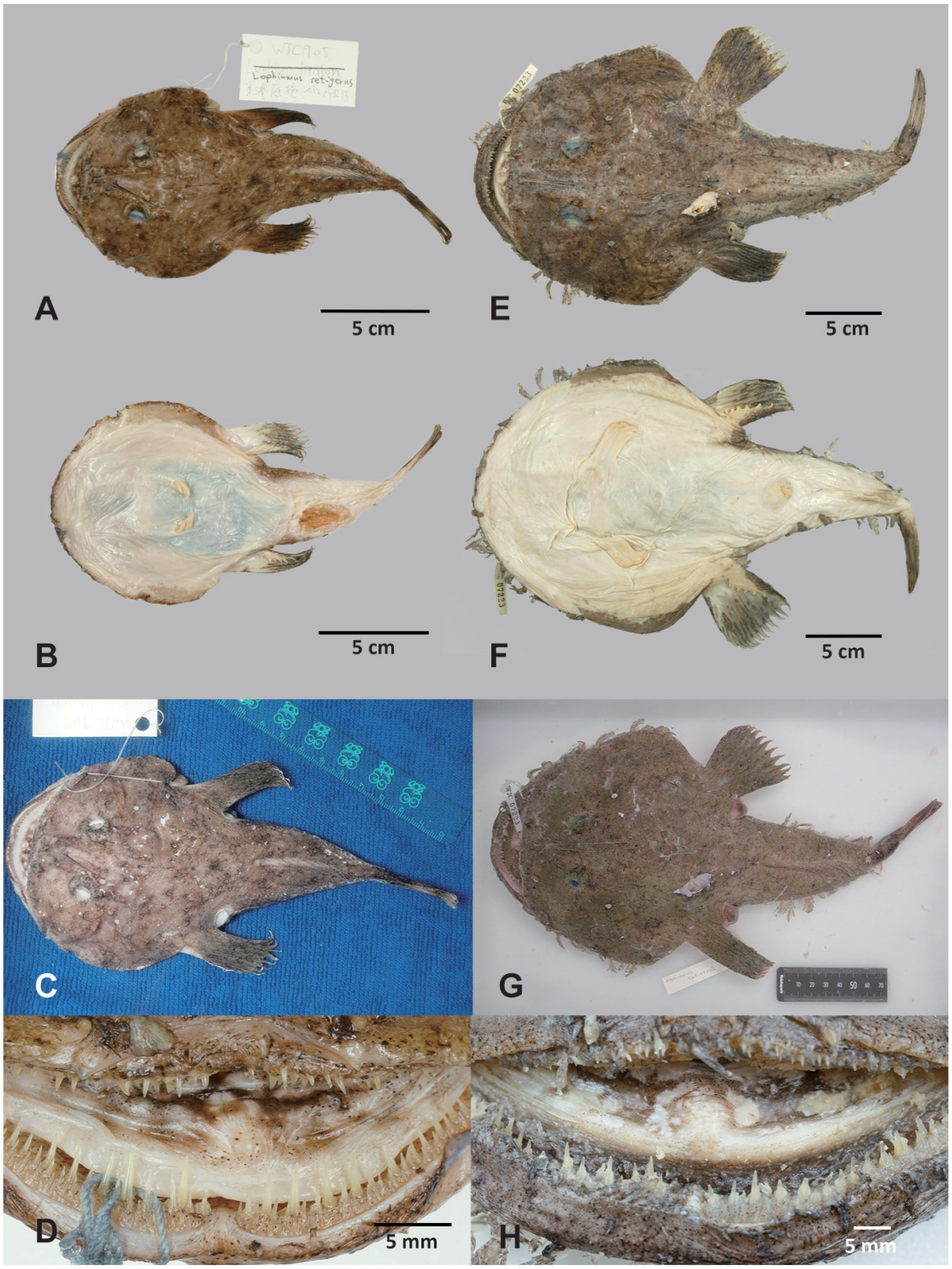

Fig. 8. *Lophiomus setigerus* (Vahl, 1797). **A–D**. Neotype (NTUM10408, sample ID: WJC0905). **E–H**. Large specimens (NTUM14414, sample ID: WJC7223). **A**. Preserved specimen, dorsal view. **B**. Ditto, ventral view. **C**. Ditto, fresh specimen. **D**. Ditto, floor of mouth. **E**. Preserved specimen, dorsal view. **F**. Ditto, ventral view. **G**. Ditto, fresh specimen. **H**. Ditto, floor of mouth.

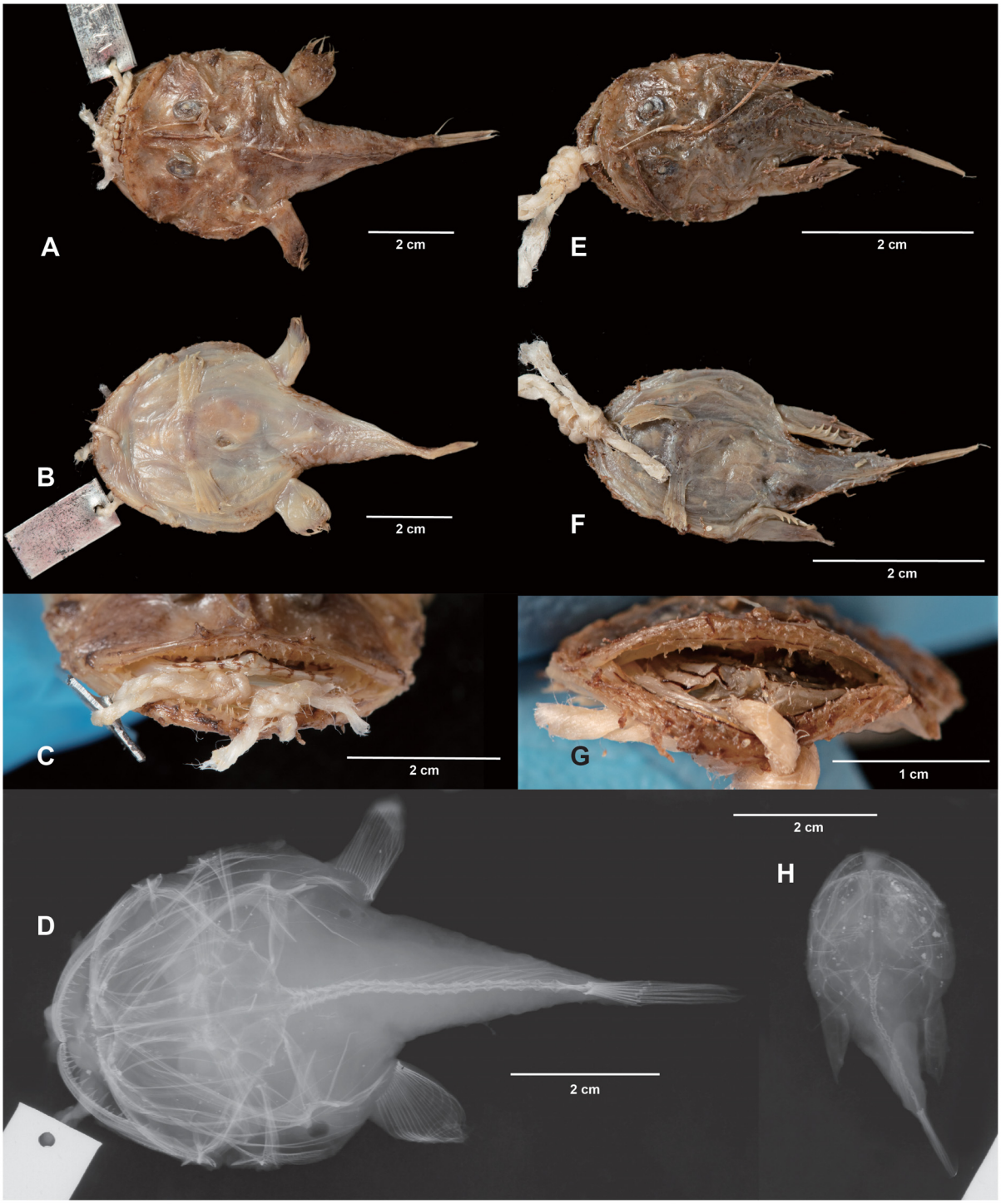

Fig. 9. *Lophius indicus* Alock, 1889. **A–D**. Large syntype (BMNH 1890.11.28.45). **E–H**. Small syntype (BMNH 1890.11.28.45.46). **A**. Preserved specimen, dorsal view. **B**. Ditto, ventral view. **C**. Ditto, floor of mouth. **D**. Ditto, X-ray radiograph. **E**. Preserved specimen, dorsal view. **F**. Ditto, ventral view. **G**. Ditto, floor of mouth. **H**. Ditto, X-ray radiograph. Photographed by L. Goodayle.

spines sharp, with posterior one stronger; frontal ridges and outer surface of maxilla, dentary bones bearing low and conical knobs; hyomandibular and symplectic bones sometimes rugose; frontal spines blunt, with posterior one sharper and stronger; inner sphenotic spines blunt; outer sphenotic spines blunt, stronger than inner one; pterotic spines low, broad, and blunt; parietal, epiotic, and posttemporal spines short and blunt, inconspicuous; articular spines strong and sharp, with single spine anterior to jaw joint; quadrate spines strong and blunt; hyomandibular spines blunt; opercular spines blunt; interopercular spines strong and blunt; subopercular spines strong; cleithral spines strong; humeral spines well developed, with three to four sharp spinelets at its tip; edge of head and caudal peduncle covered by black tendrils.

Fins. Illicium moderate to long (21.4%–32.7% SL, mean 26.2 ± 0.03%), without tendrils and reaching beyond basal ⅓ of retracted third dorsal-fin spine; esca ranges from pennant-like flap to flag-like tassel, with cirri, sometimes with one or two dark, stalked, bulb-like appendages at base; second dorsal-fin spine short (15.0%–25.7% of SL, mean 18.7 ± 0.03%), stout, reaching between parietal spines and base of third dorsal-fin spine, with dark tendrils; third dorsal-fin spine short (16.3%–25.5% of SL, mean 21.8± 0.02%), slender, reaching from about ½ of retracted fourth dorsal-fin spine, base imbedded under skin, with dark tendrils; fourth dorsal-fin spine slender, about basal ⅓ imbedded under skin and with dark tendrils, reaching from fifth dorsal-fin spine to origin of dorsal-fin; fifth and sixth dorsal-fin spines short, mostly imbedded under skin and with dark tendrils; first dorsal-fin ray relatively close to second, both imbedded under skin, last two rays short.

Coloration (preserved). Body color ranges from uniformly grayish to reddish brown, covered by scarce blackish brown spots on dorsal surface; ventral surface pale, with peritoneum gray; floor of mouth dark, with circular light pattern in smaller specimens, but irregular light pattern in larger specimens; dorsal surface of pectoral-fins dark apically, and pigmented as adjacent area of body basally; dorsal-fin pale; caudal fin dark basally and apically, with color pattern same as adjacent area of body.

Coloration (fresh). Similar to preserved coloration, but body color sometimes blackish brown.

Distribution

Northwest Pacific, East China Sea, South China Sea, Timor Sea, and adjacent to Japan, China, Taiwan, and western Australia (this study, Fig. 1). It should be noted that the previously recorded '*Lm. setigerus*' from the eastern coast of Australia (Caruso 1983), New Caledonia (Kulbicki *et al.* 1994; Ho & Chen 2013), and the Indian Ocean (Caruso 1983) should belong to different species according to our phylogenetic and species delimitation results. Thus, previous distribution records of *Lm. setigerus* from the localities above are considered doubtful and not included in this study. Due to limited sampling, records from the East Pacific (Mexico) (De La Cruz-Agüero *et al.* 1994; Love *et al.* 2021), Red Sea (Khalaf 2004; Golani & Bogorodsky 2010), and Africa (Bianchi 1985; Caruso 1986; Fischer *et al.* 1990; Sommer *et al.* 1996) could not be confirmed and are not included in this study either.

Remarks

The type specimens of the species described by Vahl (1797), including *Lophius setigerus* (= *Lm. setigerus*) and *Lophius stellatus* (= *Halieutaea stellata*, Ogcocephalidae), have never been designated or located (Fricke *et al.* 2022; R. Fricke pers. com.). Although Fricke *et al.* (2022) reported one skeleton (AMS I.25832-004) as a possible syntype of *Lm. setigerus* (locality: Australia), this specimen has apparently been lost (not held in AMS; A. Hay pers. com.) and was not collected from a locality close to the distribution center of *Lm. setigerus* inferred in this study. We feel that it is necessary and justifiable to propose a neotype for *Lm. setigerus* to avoid taxonomic confusion.

Accordingly, a specimen (NTUM10408, sample ID: WJC0905) collected from the Taiwan Strait (off Donggang, Pingtung County, Taiwan), an area that could be encompassed within the type locality of *Lm. setigerus* – broad sense of 'China' in the 18th century – is designated here as the neotype for *Lm. setigerus*.

This specimen aligns with the original description of *Lm. setigerus* on the pattern of the floor of the mouth and general appearance (Table 1; Fig. 8D) (Vahl 1797). Although the original description of *Lm. setigerus* implied a pectoral-fin rays count of 10 ("*Pinnae pectorales ..., decem-radiatae* [Pectoral-fin…ten-radiated]"; Vahl 1797: 216), this count is distinct from the currently described species of *Lophiomus*, which typically have more than 21 rays. The discrepancy between the original and present descriptions may be attributed to limitations in microscope and X-ray techniques during that period. Therefore, the meristic counts from the original description are considered unreliable and incomparable.

The name "*Lophius viviparus*" was introduced as an unexplained new name for *Lm. setigerus,* lacking a voucher specimen designation. It is only accompanied by a brief description "*L. Setigerus, Wahl in Skrivter af Naturh. …Habitat mare Sinense* [living in Chinese sea]" (Bloch & Schneider 1801: 142). Fricke *et al.* (2022) consequently considered this name as an objective synonym.

Lophiomus longicephalus (for which the type material has also been lost and was thus not examined in this study) (Fricke *et al.* 2022) was treated as a junior synonym of *Lm. setigerus* by Caruso (1983). Morphologically, it resembles *Lm. setigerus* based on the original description, sharing characteristics such as a brown body coloration, a dark floor of the mouth pattern with white spots, and an overlapped distribution (Table 1). Herein, its synonym status is confirmed.

Regarding *Lophius indicus*, its syntypes share morphological features with *Lm. setigerus,* both displaying a brown body color (Fig. 9A, E), a dark floor of the mouth with circular light patterns (Fig. 9C, G), and 22–23 pectoral-fin rays (Table 5). However, advanced morphological diagnoses are impeded by a lack of a direct morphometric comparison between *Lm. setigerus* and *Lp. indicus* due to relatively smaller size of the available *Lp. indicus* syntypes (SL = 35.3–66.4 mm) (Tables 3–4). Along with its morphological similarity between *Lm*. *setigerus* and the lack of further evidence, the synonym status of *Lp. indicus* with *Lm. setigerus* suggested by Caruso (1983) is remained.

Chirolophius malabaricus is another synonym of *Lm. setigerus* (Caruso 1983). It was described based on the specimens collected from the Malabar Coast of southwestern India. Since a considerable geographical isolation to either *Lp. indicus* (type locality: Bay of Bengal) or *Lm. setigerus* (West Pacific), and a higher count of pectoral-fin rays than other congeners (24 vs 21–23, mostly 22) (Tables 1, 3), we opine that *C. malabaricus* could potentially be a distinct species of *Lophiomus* that should be excluded from the synonymy of *Lm. setigerus*. However, the absence of a type examination of *C. malabaricus* and the lack of direct genetic evidence (aside from our discussions on GenBank sequences of "*Lp. indicus*") prevent us from formally resurrecting this nominal species. Therefore, we tentatively consider it as incertae sedis.

Lophiomus laticeps (Ogilby, 1910) stat. rev.
urn:lsid:zoobank.org:act:4226D3F2-F927-4460-A63D-DABBDDA14E34
Figs 10–11, 15B, 16A–B; Tables 3–6

Chirolophius laticeps Ogilby, 1910: 136.

Lophiomus setigerus (not Vahl, 1797) – Caruso 1983: 13 (in part).

Diagnosis

This species can be separated from other congeners by the combination of dorsal-fin spines 6, pectoral-fin rays 24–25, pelvic-fin rays 7, pale khaki body coloration, and light floor of mouth having anastomosing dark pattern medially.

Differential diagnosis

Lophiomus laticeps resembles *Lm. nigriventris* sp. nov. according to their shared pale khaki body coloration. However, notable distinctions include higher counts of pectoral-fin rays (24–25 vs 23–24, mostly 23 in *Lm. nigriventris* sp. nov.; Table 6) and pelvic-fin rays (7 vs 6 in *Lm. nigriventris*), longer DS2 (17.4–25.5% SL vs 17.9–20.7% SL in *Lm. nigriventris*) and DS3 (27.3–33.7% SL vs 18.9–24.0% SL in *Lm. nigriventris*), narrower ISP (39.2–39.9% HL vs 40.6–45.4% HL in *Lm. nigriventris*), tassel-like flap of esca (pennant-like in *Lm. nigriventris*), a peritoneum without dark or gray pigmentation (with dark pigmentation in *Lm. nigriventris*), and a light floor of the mouth having anastomosing dark pattern medially (light floor of the mouth with reticulate dark pattern in *Lm. nigriventris*).

This species is also different from the sympatric species *Lm. carusoi* sp. nov. in having higher counts of pectoral-fin rays (24–25 vs 23–24 in *Lm. carusoi*), a relatively longer (HL 34.2–39.9% SL vs 28.4–32.7% SL in *Lm. carusoi*) and a narrower head (HW 50.7–54.3% HL vs 58.1–68.6% HL in *Lm. carusoi*), a narrower ISP (39.2–39.9% HL vs 48.6–56.7% HL in *Lm. carusoi*), and shorter OPSOP (31.6–47.4% HL vs 55.5–65.7% HL in *Lm. carusoi*), a pale khaki body coloration (brown in *Lm. carusoi*), a peritoneum without dark or gray pigmentation (with dark pigmentation in *Lm. carusoi*), and a light floor of the mouth having an anastomosing dark pattern medially (light floor of the mouth with reticulate dark pattern in *Lm. carusoi*).

Lastly, this species is different from the type species *Lm. setigerus* in having higher counts of pectoral-fin rays (24–25 vs 21–23 in *Lm. setigerus*), pale khaki body coloration (brown in *Lm. setigerus*), peritoneum without dark pigmentation (with gray pigmentation in *Lm. setigerus*), and a light floor of the mouth having anastomosing dark pattern medially (dark floor of the mouth with circular or irregular light pattern in *Lm. setigerus*).

Material examined

Holotype

CORAL SEA • 145.1 mm SL (currently measured); West Pacific, Coral Sea, Moreton Bay, 58 km northeast off Cape Moreton; 27°10′ S, 153°17′ E; 133.5 m (73 fathoms) deep; 6 Jul.–13 Sep. 1910; F.I.S. “Endeavour”; trawl; Voucher: AMS E. 2973.

Non-type material

CORAL SEA • 237.1 mm SL, sample ID: NC1375; West Pacific, Coral Sea, SW of New Caledonia, north of Lord Howe seamount chain, Nova Bank, stn CP5004; 159°25′ E, 22°40′ S; 340 m deep; 18 Sep. 2017; R/V *ALIS*; French beam trawl; KANADEEP exped.; GenBank nos: OR261070 (*COI*), OR257541 (*cytb*), OR260587 (*rhodopsin*), OR257563 (*RAG1*); Voucher: NTUM13463 • 152.8 mm SL, sample ID: NC964; West Pacific, Coral Sea, SW of New Caledonia, North of Lord Howe seamount chain, Capel Bank, stn CP4930; 159°55’E, 25°08’S; 300 m deep; 3 Sep. 2017; R/V *ALIS*; French beam trawl; KANADEEP expedition; GenBank nos: OR261071 (*COI*), OR257542 (*cytb*), OR260586 (*rhodopsin*), OR257562 (*RAG1*); Voucher: NTUM13468.

Redescription

Adult

Measurements and meristic counts. Morphometric values given in Tables 3 and 4. Dorsal-fin spines 6; dorsal-fin rays 8, double-forked in last ray; anal-fin rays 6; pectoral-fin rays 23–25; pelvic-fin rays 7; branchiostegal rays 5; interopercular spines 2; vertebrae 18–19; outermost row of premaxillary teeth 15–22 (Tables 5–6).

Head and body. Head relatively long (34.2%–39.9% of SL) and narrow (50.7%–54.3% of HL); eyes suboval; anterior half of premaxilla with three rows of enlarged teeth with largest on innermost row,

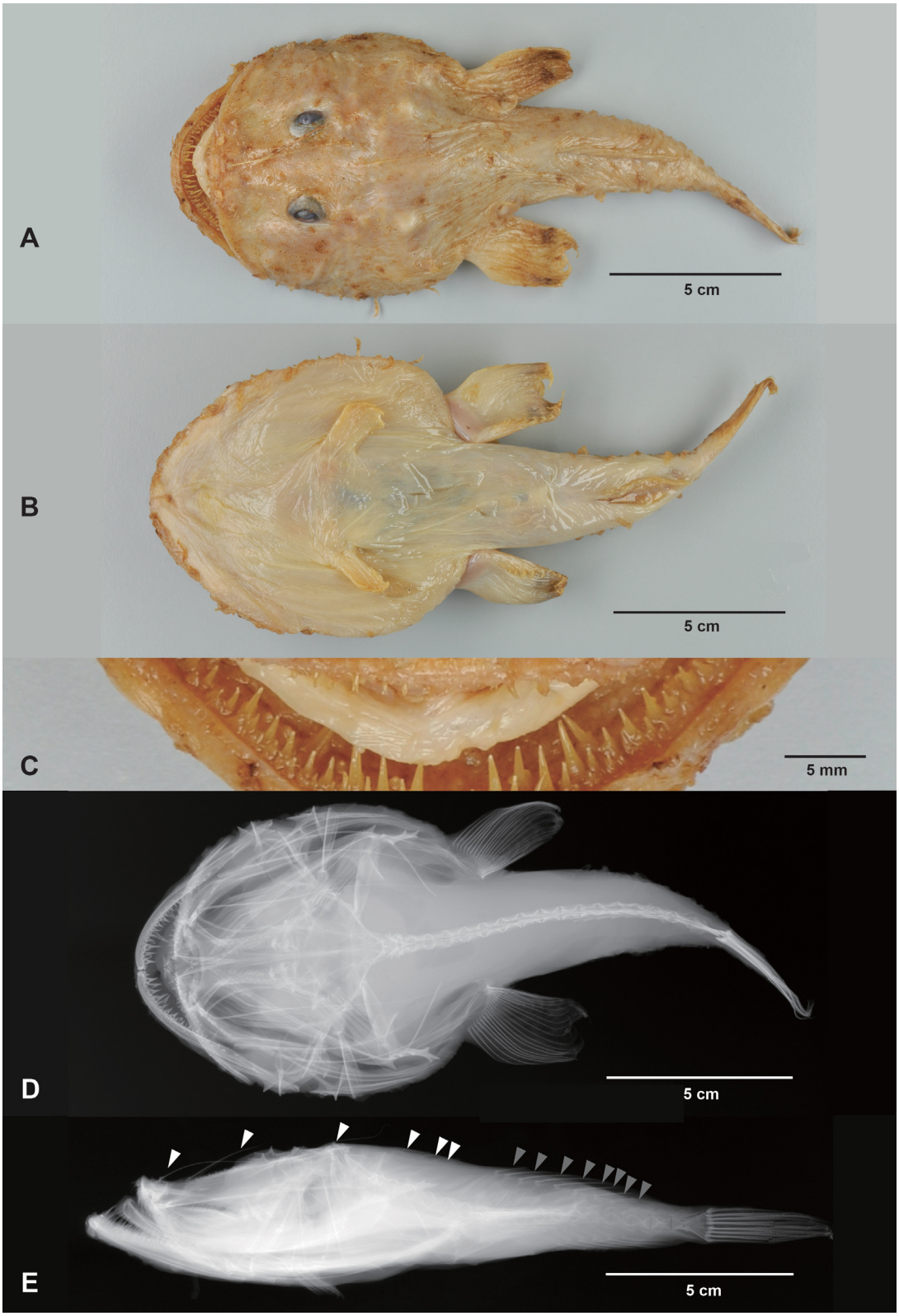

Fig. 10. *Chirolophius laticeps* Ogilby, 1910, holotype (AMS E. 2973). **A**. Preserved specimen, dorsal view. **B**. Ventral view. **C**. Floor of mouth. **D**. X-ray radiograph in dorsal view. **E**. X-ray radiograph in lateral view (white triangles indicate the dorsal-fin spines; gray triangles indicate the dorsal-fin rays). Photographed by K. Parkinson.

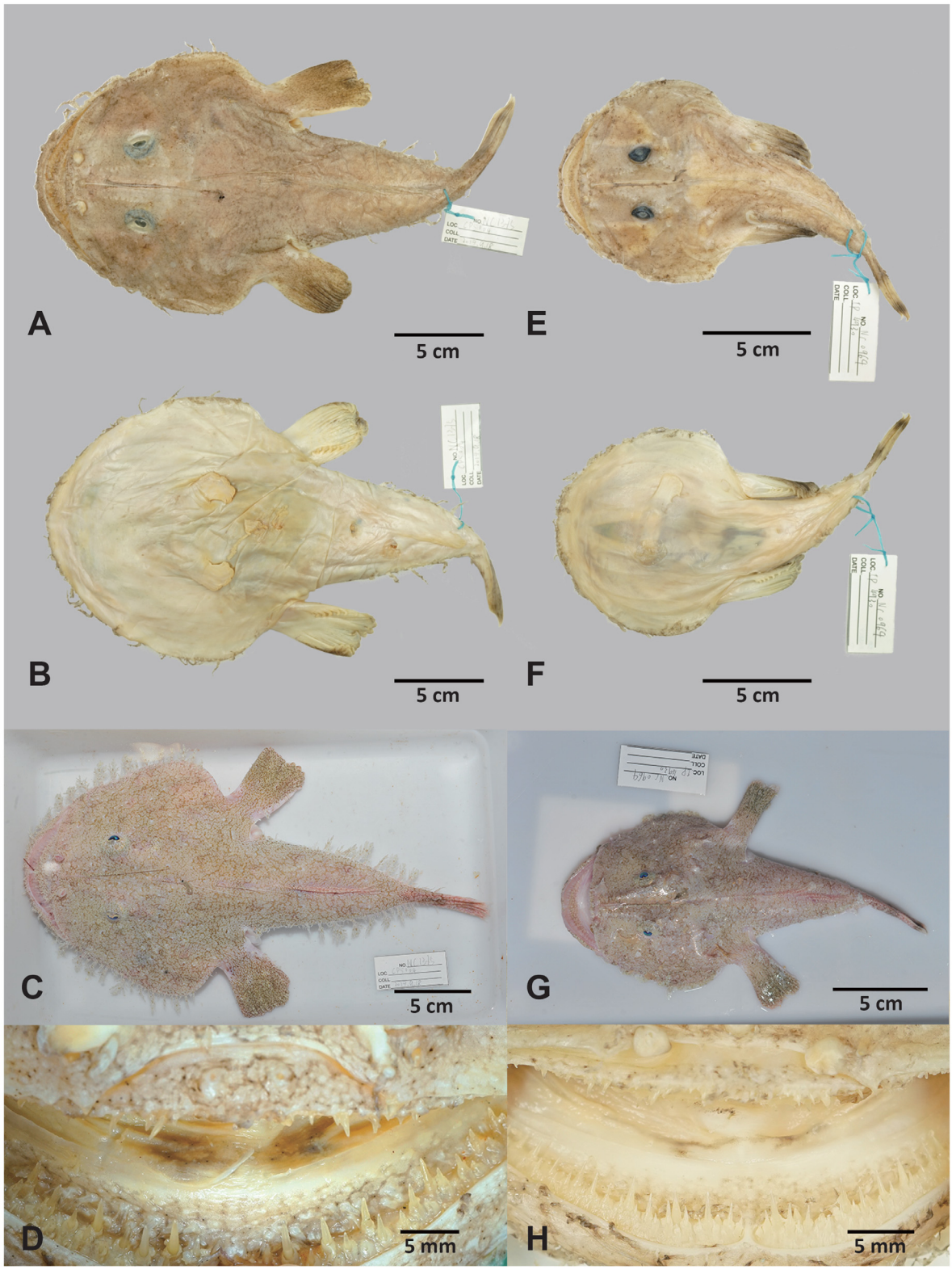

Fig. 11. *Lophiomus laticeps* stat. rev., newly collected specimens. **A–D**. Large (NTUM13463, sample ID: NC1375). **E–H**. Small (NTUM13468, sample ID: NC964). **A**. Preserved specimen, dorsal view. **B**. Ditto, ventral view. **C**. Ditto, fresh specimen. **D**. Ditto, floor of mouth. **E**. Preserved specimen, dorsal view. **F**. Ditto, ventral view. **G**. Ditto, fresh specimen. **H**. Ditto, floor of mouth.

followed by single row of small teeth on posterior half; maxilla toothless; palatine with single row of small teeth with some enlarged; dentary with three rows of teeth, outer teeth minute and innermost teeth largest; fifth ceratobranchial with two rows of small teeth, forming V-shaped patch; teeth on second and third pharyngobranchials forming small and rounded patches; gill rakers and pseudobranch absent. Palatine spines sharp, with posterior one stronger; frontal ridges and outer surface of maxilla, dentary bones bearing low and conical knobs; frontal spines blunt, with posterior one sharper; inner sphenotic spines low and blunt; outer sphenotic spines blunt, stronger than inner one; pterotic spines broad and blunt; parietal, epiotic, posttemporal spines short and blunt, inconspicuous; articular spines strong and sharp, with single spine anterior to jaw joint and projected forward; quadrate spines strong and sharp; hyomandibular spines blunt; opercular spines blunt; interopercular spines strong and sharp; subopercular spines blunt, with posterior one inconspicuous; cleithral spines strong and blunt; humeral spines well developed, with three to four sharp spinelets at tips; edge of head and caudal peduncle covered by pale tendrils.

Fins. Illicium moderate to long (23.3%–31.3% of SL), without tendrils; esca tassel-like flap with moderately long cirri and two dark, stalked, bulb-like appendages at base of esca in larger specimen; second dorsal-fin spine long (17.4%–25.5% of SL), stout, reaching between base of third dorsal-fin spine and epiotic spines, with dark tendrils; third dorsal-fin spine relatively long (27.3%–33.7% of SL), slender, reaching from about ¾ fourth dorsal-fin spine, without tendrils; fourth dorsal-fin spine slender, with sparse or without tendrils; fifth and sixth dorsal-fin spines short, mostly imbedded under skin and with dark tendrils; first dorsal-fin ray relatively close to second, both imbedded under skin, last two rays short; anterior three anal-fin rays imbedded under skin.

Coloration (preserved). Body color gray khaki, covered by sparse, circular dark marking (holotype only), dense, minute pale spots and blackish-brown irregular reticulate pattern on dorsal surface; ventral surface and peritoneum pale; floor of mouth light with anastomosing dark pattern in middle, obvious in larger specimen; dorsal surface of pectoral-fins dark apically, and pigmented as adjacent area of body basally; dorsal-fin pale; caudal fin dark basally and apically, with color pattern same as adjacent area of body.

Coloration (fresh). Body color pale khaki, covered by pale spots and blackish-brown irregular reticulate pattern on dorsal surface; dorsal surface of pectoral-fins brown with color pattern same as adjacent area of body basally; dorsal-fin and caudal fin pink covered by circular pale spots densely, brownish basally on caudal fin, with color pattern same as adjacent area of body.

Subadult

Unknown.

Distribution

Coral Sea, Moreton Bay at a depth of 133.5 m (holotype); Lord Howe seamount chain (Nova Bank and Capel Bank) at depths of 300 m and 340 m (two adult specimens) (this study, Fig. 1).

Remarks

The holotype of *C. laticeps* and two specimens collected from Lord Howe seamount chain are considered conspecific since their morphological similarities including pale khaki body coloration, 24 pectoral-fin rays, 7 pelvic-fin rays, and anastomosing dark pattern on the floor of the mouth (Figs 10–11; Table 5). As the holotype of *C. laticeps* was examined by Caruso, this species falls within the morphological variation of *Lm. setigerus* sensu Caruso (1983).

This species is partially sympatric with another Australian species, *Lm. carusoi* sp. nov. (Fig. 1). However, the distinction in morphology and genetics (Figs 2, 10–11, 14; Table 7), as well as their non-sister relationship (Figs 2–4), support the absence of a genetic flow between these two species.

Lophiomus immaculioralis sp. nov.
urn:lsid:zoobank.org:act:F6FE6067-613F-41C5-8C0E-7750F473F7EE
Figs 12, 15C, 16D; Tables 3–6

Diagnosis

This new species can be separated from other congeners by the combination of dorsal-fin spines 5, pelvic-fin rays 7, pectoral-fin rays 21–22, OPSOP 22.2% of HL, brown body coloration, and the absence of conspicuous dark marking on the light floor of the mouth.

Differential diagnosis

Lm. immaculioralis sp. nov. is most similar to its sister species *Lm. setigerus* in brown body coloration and pectoral-fin ray counts but differs in having a lower count of dorsal-fin spines (5 vs 6 in *Lm. setigerus*), shorter OPSOP (22.2% HL vs 46.1–60.0% HL in *Lm. setigerus*), a tassel-like flap esca (mostly pennant-like in *Lm. setigerus*), and a peritoneum without dark or gray pigmentation (gray in *Lm. setigerus*).

Since this new species is described based on a single specimen, the molecular differential diagnosis between the two species at *COI* gene level shown below is especially provided for aiding species identification: Nos. 45 (T vs C), 87 (G vs A), 90 (G vs A), 102 (T vs C), 103 (T vs C), 105 (A vs G), 106 (G vs C), 168 (T vs C), 177 (A vs G), 204 (C vs T), 207 (G vs A), 210 (C vs T), 255 (A vs G), 273 (C vs T), 282 (C vs T), 337 (C vs T), 348 (A vs G), 363 (G vs A), 369 (T vs C), 372 (G vs A), 453 (C vs T), 522 (A vs G), 555 (G vs A), 558 (G vs A), 561 (C vs T), 585 (T vs A), 618 (T vs C). Numbering of the position starts from the first nucleotide site of the gene. The differences can translate into a 4.9% sequence divergence.

Etymology

The name *immaculioralis* is derived from the Latin '*immaculi-*' (meaning 'unstained') plus '*oralis*' (meaning 'oral'). It refers to the floor of the mouth in this species being light, without conspicuous dark pigmentation.

Material examined

Holotype

ANDAMAN SEA • 243.0 mm SL, sample ID: WJC7777; Thailand, Ranong, Ranong fish landing port; ca 100–200 m deep; 21 Mar. 2018; GenBank nos: OR261060 (*COI*), OR257552 (*cytb*), OR260579 (*rhodopsin*), OR257564 (*RAG1*); Voucher: NTUM16313.

Description

Adult

Measurements and meristic counts. Morphometric values given in Tables 3 and 4. Dorsal-fin spines 5; dorsal-fin rays 8; anal-fin rays 6; pectoral-fin rays 21–22; pelvic-fin rays 7; branchiostegal rays 5; quadrate spine 1; interopercular spines 2; vertebrae 19; outermost row of premaxillary teeth 33–35 (Tables 5–6).

Head and body. Head relatively short (31.9% of SL) and narrow (54.9% of HL); eyes suboval; anterior half of premaxilla with three rows of enlarged teeth, largest on innermost row followed by single row of small teeth on posterior half; maxilla toothless; palatine with single row of small teeth, with some enlarged; dentary with three rows of teeth, outer teeth minute, and innermost teeth largest; fifth ceratobranchial with two rows of small teeth, forming V-shaped patch; teeth on second and third pharyngobranchials

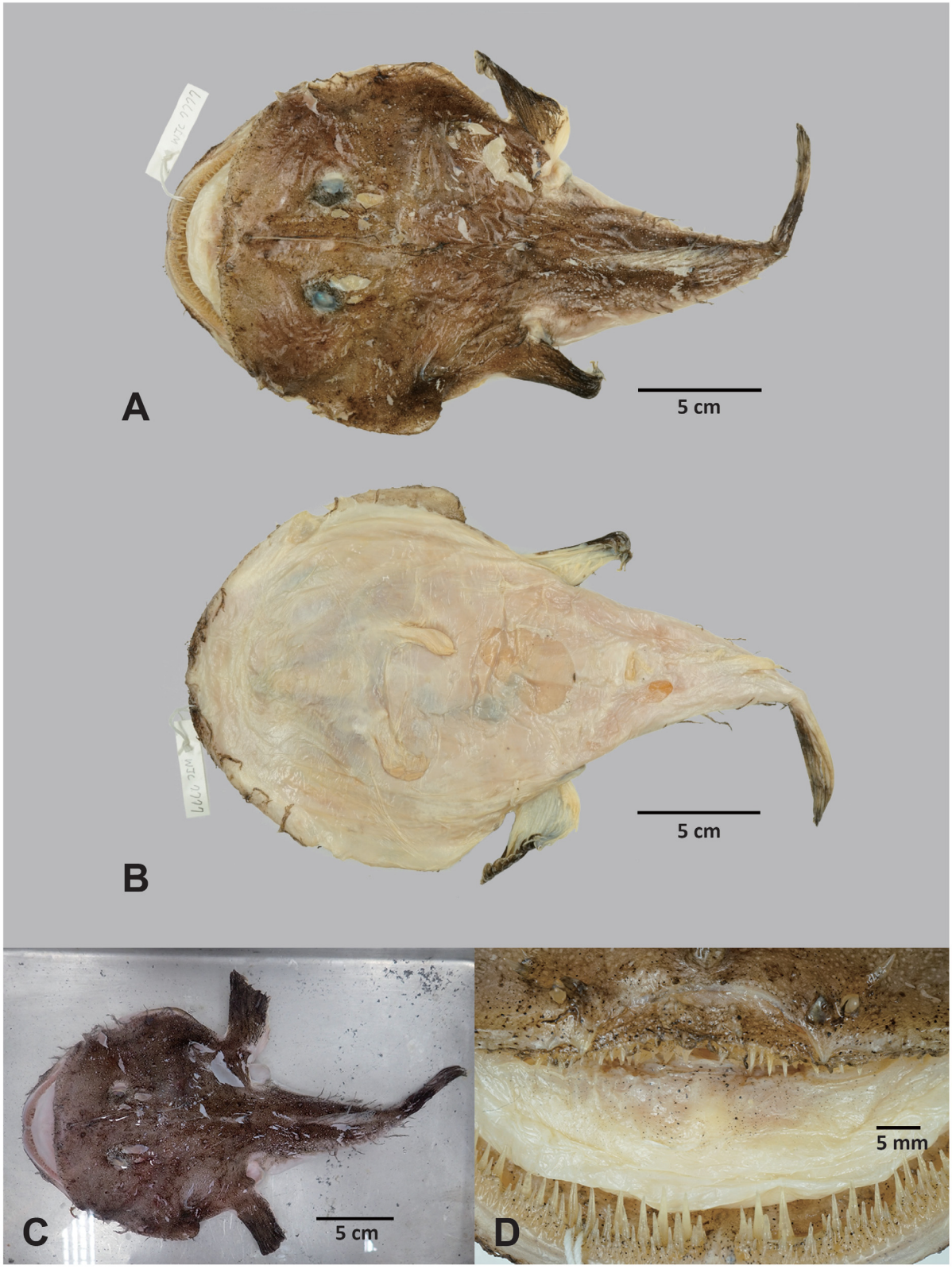

Fig. 12. *Lophiomus immaculioralis* sp. nov., holotype (NTUM16313, sample ID: WJC7777). **A**. Preserved specimen, dorsal view. **B**. Ditto, ventral view. **C**. Ditto, fresh specimen. **D**. Ditto, floor of mouth.

forming small and rounded patches; gill rakers and pseudobranch absent. Palatine spines sharp, with posterior one stronger; frontal ridges and outer surface of maxilla, dentary, and quadrate bones bearing low and conical knobs; frontal spines sharp, with posterior one sharper, stronger, and bearing small knobs; inner sphenotic spines blunt, low, and broad; outer sphenotic spines sharp and strong; pterotic, parietal, epiotic, and posttemporal spines low, broad, and blunt; articular spines sharp and strong, with single spine anterior to jaw joint; quadrate spines sharp and strong; hyomandibular spines low but sharp; opercular spines blunt, low, and broad; interopercular and subopercular spines strong and sharp; cleithral spines strong; humeral spines well developed, with five sharp spinelets at tips; edge of head and caudal peduncle covered by black tendrils.

Fins. Illicium short (30.7% of SL), without tendrils and reaching basal ⅓ of retracted third dorsal-fin spine; esca tassel-like flap with long dark cirri; second dorsal-fin spine relatively short (18.3% of SL), slender, reaching position of inner sphenotic spines, with dark tendrils; third dorsal-fin spine relatively short (23.5% of SL), pale and slender, reaching from about ⅓ of retracted fourth dorsal-fin spine, without tendrils; fourth dorsal-fin spine pale, slender, without tendrils; fifth dorsal-fin spine long, mostly imbedded under skin; sixth dorsal-fin spine absent; posterior dorsal-fin rays shorter than anterior.

Coloration (preserved). Body color reddish brown, uniformly covered with irregularly shaped pale spots on dorsal surface, denser in caudal peduncle; ventral surface pale, with peritoneum light; floor of mouth light, without conspicuous dark marking, with minute dark spot scarcely; dorsal surfaces of pectoral-fins dark apically and pigmented as adjacent area of body basally; dorsal-fin and dorsal-fin rays pale; caudal fin dark basally and apically, with color pattern same as adjacent area of body.

Coloration (fresh). Same as preserved coloration.

Subadult

Unknown.

Distribution

Andaman Sea, waters off Ranong, Thailand (holotype) (this study, Fig .1).

Remarks

Comparing with two previously described nominal species of *Lophiomus* that are also distributed in the Indian Ocean, namely *Lp. indicus* and *C. malabaricus*, this new species is different from both by having floor of mouth without conspicuous dark marking (black with circular white patches in *Lp. indicus*, unknown in *C. malabaricus*), lower pectoral-fin ray count (21–22 vs 22–23 in *Lp. indicus*, 24 in *C. malabaricus*), and lower dorsal-fin spine count (5 vs 6 in both nominal species) (Figs 9C, G, 12D; Tables 1, 5). Given the non-overlapping distribution between two nominal species (Andaman Sea off Ranong vs Bay of Bengal, for *Lp. indicus* and Kerala coast, southwest India, for *C. malabaricus*) (Fig. 1; Table 1), along with substantial genetic differences (16.1% at *COI* gene) to '*Lp. indicus*' (Table 7; Fig. 2) and the mentioned morphological distinctions, this new species is considered a distinct species from the two nominal species from the Indian Ocean.

Lophiomus nigriventris sp. nov.
urn:lsid:zoobank.org:act:9F783F26-5547-4346-8C08-3B1B59B8DB31
Fig. 13, 15D, 16C; Tables 3–6

Lophiomus setigerus (not Vahl, 1797) – Caruso 1983: 13 (in part).

Diagnosis

This new species can be separated from other congeners by the combination of dorsal-fin spines 6, pelvic-fin rays 6, pectoral-fin rays 23–24, pale khaki body coloration, peritoneum with dark pigmentation, and reticulate dark pattern on the light floor of the mouth.

Differential diagnosis

Lophiomus nigriventris sp. nov. closely resembles its sibling, *Lm. carusoi* sp. nov., in terms of pectoral-fin ray counts, peritoneum pigmentation, and the pattern on the floor of the mouth. However, distinctions include the absence of cirri in the pennant-like esca flap (tassel-like or pennant-like flap with moderately long cirri in *Lm. carusoi*), a shorter DS4 (8.4–17.3% SL vs 16.7–24.0% SL in *Lm. carusoi*), a narrower SNW (31.8–39.5% HL vs 41.9–55.7% HL in *Lm. carusoi*), ISP (40.6–45.4% HL vs 48.6–56.7% HL in *Lm. carusoi*) and OPSOP (47.3–53.6% HL vs 55.5–65.7% HL in *Lm. carusoi*).

Furthermore, this newly described species can be distinguished from the potential sympatric species *Lm. setigerus* by its pale khaki body coloration (brown in *Lm. setigerus*), a dark peritoneum (gray in *Lm. setigerus*), and the light floor of the mouth with a reticulate dark pattern (dark floor of the mouth with circular or irregular light patterns in *Lm. setigerus*).

Etymology

The name *nigriventris* is derived from the Latin '*niger*' (meaning 'black') plus '*venter*' (meaning 'belly'). It refers to the black peritoneum of the adult.

Material examined

Holotype

SOUTH CHINA SEA • 193.2 mm SL, sample ID: WJC5808; West Pacific, South China Sea, Macclesfield Bank, stn CP4149; 114°23′ E, 16°07′ N; 162–165 m deep; 26 Jul. 2015; RV *Ocean Researcher 1*; beam trawl; ZhongSha 2015 exped.; GenBank nos: OR263455 (*COI*), OR257536 (*cytb*), OR260588 (*rhodopsin*); Voucher: NTUM15096.

Paratypes

WETERN PACIFIC • 34.8 mm SL, sample ID: PNG3184; Papua New Guinea, north off Kavieng, stn CP4457; 150°41′ E, 02°33′ S; 133–178 m deep; 2 Sep. 2014; RV *ALIS*; beam trawl; KAVIENG 2014 exped.; GenBank nos: OR263441 (*COI*), OR257534 (*cytb*), OR260577 (*rhodopsin*), OR257555 (*RAG1*); Voucher: NTUM12188.

SOUTH CHINA SEA • 147.4 mm SL, sample ID: WJC5708; Northwestern Pacific, South China Sea, W of Luzon Island, Macclesfield Bank of Zhongsha Atoll, stn CP4146: 114°16′ E, 16°09′ N; 232–314 m deep; 26 Jul. 2015; RV *Ocean Researcher 1*; beam trawl; ZhongSha 2015 exped.; GenBank nos: OR263450 (*COI*), OR257537 (*cytb*); Voucher: NTUM15094 • 220.8 mm SL, sample ID: WJC5709; same data as for preceding; Voucher: NTUM15094 • 185.0 mm SL, sample ID: WJC5796; same data as for preceding, stn CP4148; 114°19′ E, 16°07′ N; 218–281 m deep; 26 Jul. 2015; Voucher: NTUM15094 • 189.7 mm SL, sample ID: WJC5807; same data as for preceding; GenBank no.: OR263453 (*COI*); Voucher: NTUM15095 • 192.1 mm SL, sample ID: WJC5809; same data as for preceding, stn CP4149; 114°23′ E, 16°07′ N; 162–165 m deep; 26 Jul. 2015; GenBank no.: OR263454 (*COI*); Voucher: NTUM15096.

Description

Adult

Measurements and meristic counts. Morphometric values given in Tables 3 and 4. Dorsal-fin spines 6; dorsal-fin rays 8; anal-fin rays 6; pectoral-fin rays 23-24; pelvic-fin rays 6; branchiostegal rays 5; quadrate spine 1; interopercular spines 2; vertebrae 18; outermost row of premaxillary teeth 17–24 (Tables 5–6).

Head and body. Head relatively short (28.8%–33.3% of SL, mean 30.9 ± 0.02%) and wide (52.8%–62.0% of HL, mean 57.8 ± 0.03%); eyes suboval; anterior half of premaxilla with three rows of enlarged

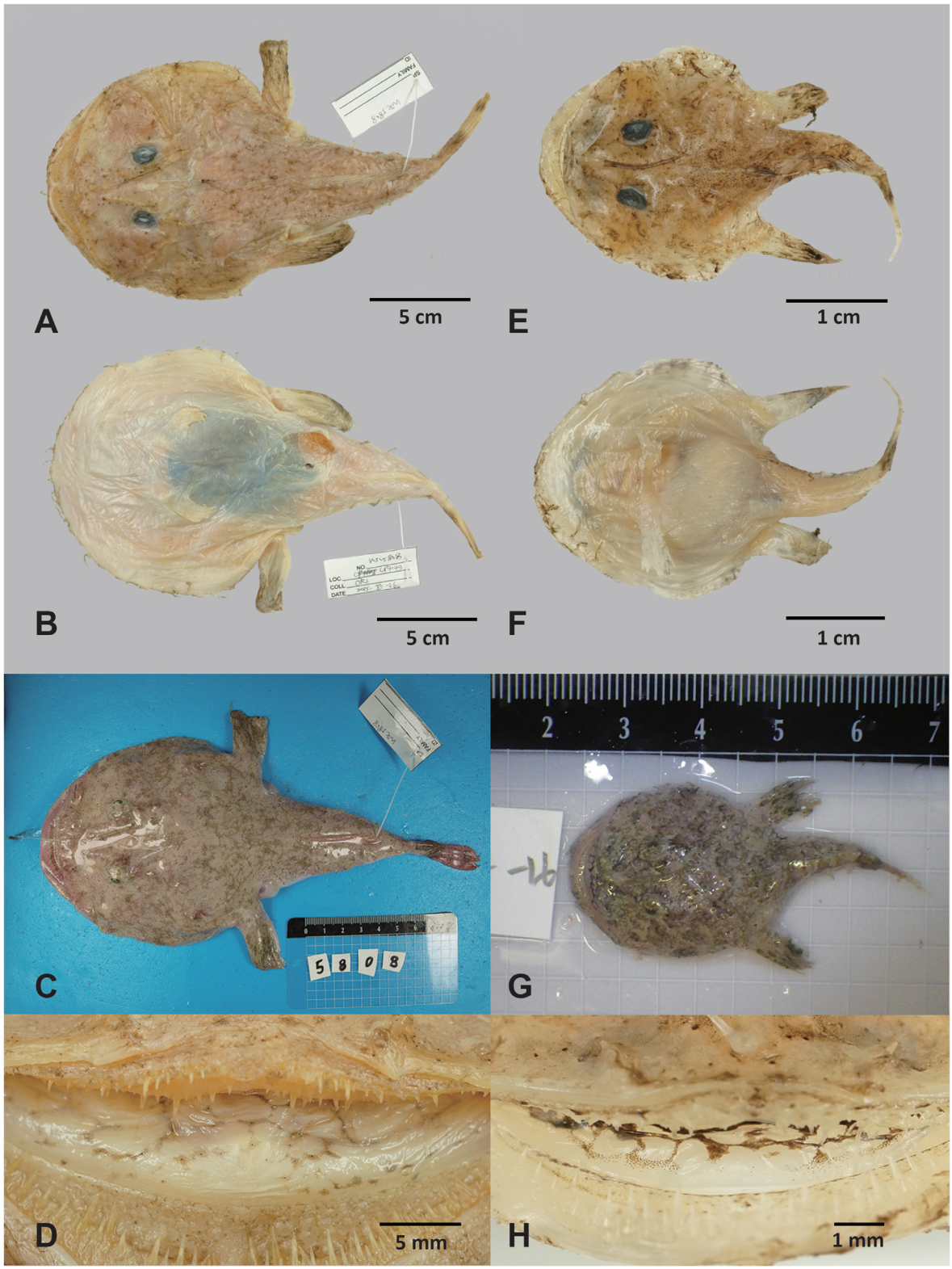

Fig. 13. *Lophiomus nigriventris* sp. nov. **A–D**. Holotype (NTUM15096, sample ID: WJC5808). **E–H**. Subadult paratype (NTUM12188, sample ID: PNG3184). **A**. Preserved specimen, dorsal view. **B**. Ditto, ventral view. **C**. Ditto, fresh specimen. **D**. Ditto, floor of mouth. **E**. Preserved specimen, dorsal view. **F**. Ditto, ventral view. **G**. Ditto, fresh specimen. **H**. Ditto, floor of mouth.

teeth, largest on innermost row, followed by single row of small teeth on posterior half; maxilla toothless; palatine with single row of small teeth with some enlarged; dentary with three rows of teeth, outer teeth minute and innermost teeth largest; fifth ceratobranchial with two rows of small teeth, forming V-shaped patch; teeth on second and third pharyngobranchials forming small and rounded patches; gill rakers and pseudobranch absent. Palatine spines sharp, with posterior one stronger; frontal ridges and outer surface of maxilla bones bearing low and conical knobs; frontal spines blunt, with posterior one sharper, stronger, and projected posteriorly; inner sphenotic spines low and blunt; outer sphenotic spines blunt, stronger than inner one, sometimes bearing two knobs; pterotic spines broad and blunt; parietal, epiotic, and posttemporal spines short and blunt, inconspicuous; articular spines strong and sharp, with single spine anterior to jaw joint and projected upward; quadrate spines strong and sharp; hyomandibular spines blunt; opercular spines blunt; interopercular spines strong and sharp; subopercular spines blunt, with posterior one inconspicuous; cleithral spines strong and blunt; humeral spines well developed, with three to four sharp spinelets at its tip; edge of head and caudal peduncle covered by pale tendrils.

Fins. Illicium short to moderately long (16.5%–29.0% of SL, mean 23.6 ± 0.04%), without tendrils and extending to base of third dorsal spine; esca pennant-like flap without cirri, with one or two dark, small, bulb-like appendages at base of esca; second dorsal-fin spine relatively short (17.9%–20.7% of SL, mean 19.5 ± 0.01), stout, reaching between parietal spines and base of third dorsal-fin spine, with dark tendrils; third dorsal-fin spine relatively short (18.9%–24.0% of SL, mean 21.2 ± 0.02%), slender, reaching from about ½ to ⅔ of retracted fourth dorsal-fin spine, base imbedded under skin, without tendrils; fourth dorsal-fin spine slender, about basal ⅓ imbedded under skin and with dark tendrils, reaching origin of dorsal-fin; fifth and sixth dorsal-fin spines short, mostly imbedded under skin and with dark tendrils; first dorsal-fin ray relatively close to second, both imbedded under skin, last two rays short; anterior three anal-fin rays imbedded under skin.

Coloration (preserved). Body color khaki with pink penetrates on cheeks and caudal peduncle, covered by minute pale spots densely and blackish-brown spots scarcely on dorsal surface; ventral surface pale, with peritoneum black; floor of mouth light with reticulate dark pattern; dorsal surface of pectoral-fins dark apically and pigmented as adjacent area of body basally; dorsal-fin pale; caudal fin dark basally and apically, with color pattern same as adjacent area of body.

Coloration (fresh). Body color khaki, covered by minute pale spots densely and blackish-brown pigment spots scarcely on dorsal surface; dorsal surface of pectoral-fins blackish brown with color pattern same as adjacent area of body basally; dorsal-fin pink; caudal fin dark basally and pink posterior ⅔, with color pattern same as adjacent area of body.

Subadult

Morphometric values given in Tables 3 and 4. Description similar to adult, except body color darker and with more blackish-brown pigment spots on dorsal body surface; floor of mouth with reticulate dark pattern, darker and more conspicuous than adults; peritoneum light; caudal fin pale.

Distribution

South China Sea, Macclesfield Bank at depths of 162–314 m (holotype and nine adult paratypes); West Pacific, north off Kavieng at depths of 133–178 m (one subadult paratype); Indian Ocean, waters off Exmouth Gulf at depths of 391 m and 400 m (two sequences from the BOLD systems) (this study, Fig. 1).

Remarks

This new species exhibits a potential sympatric distribution with *Lm. setigerus* (Fig. 1) and could be interpreted as an extreme manifestation of intraspecific variation within the previously defined *Lm. setigerus*, as observed by Caruso (1983). Caruso's observations include characteristics such as

"pigmentation of peritoneum variable, … dark extremely rare", and "Coloration in preserve uniform light to dark brown dorsally", along with a broad range of pectoral-fin rays (21–25; Table 5). Notably, the localities of 75% (39 of 52) of the specimens examined by Caruso (1983: 13–14) correspond to the distribution range of *Lm. setigerus* reported in this study. Additionally, the mean pectoral-fin ray count of *Lm. setigerus* sensu Caruso (1983) is 22.8, falling within the range of the currently defined *Lm. setigerus* (21–23, mostly 22). These observations suggest that the taxon described as *Lm. setigerus* sensu Caruso (1983) was mostly based on true *Lm. setigerus*, with some rare individuals displaying deviated morphologies that should be attributed to interspecific variation between *Lm. setigerus* and *Lm. nigriventris* sp. nov., as described herein.

Lophiomus carusoi sp. nov.
urn:lsid:zoobank.org:act:80F54EA1-8E6B-4C02-BC49-1D5D4A01954C
Figs 14, 15E, 16E–F; Tables 3–6

Lophiomus setigerus (not Vahl, 1797) – Caruso 1983: 13 (in part)

Diagnosis

This new species can be separated from other congeners by the combination of dorsal-fin spines 6, pelvic-fin rays 7, pectoral-fin rays 23–24, ISP 48.6–56.7% of the HL, brown body coloration, peritoneum with dark pigmentation, and reticulate pattern on the floor of the mouth.

Differential diagnosis

Lophiomus carusoi sp. nov. is most similar to its sibling species *Lm. nigriventris* sp. nov., with the distinctions highlighted in the differential diagnosis of *Lm. nigriventris*. Furthermore, it can also be differentiated from its potential sympatric species, *Lm. laticeps*, by the variations outlined previously in the differential diagnosis of *Lm. laticeps*.

Etymology

The name '*carusoi*' is a Latinized eponym honoring John Caruso, an ichthyologist who made significant contributions to the taxonomy of Lophiidae.

Material examined

Holotype

CORAL SEA • 263.5 mm SL, sample ID: NC2059; West Pacific, Coral Sea, E off New Caledonia, stn CP5131; 20°34′ S, 164°58′42″ E; 354–368 m deep; 1 Jul. 2021; GenBank nos: OR261058 (*COI*), OR257539 (*cytb*), OR260578 (*rhodopsin*), OR257554 (*RAG1*); Voucher: MNHN 2024-0099.

Paratypes

CORAL SEA • 292.5 mm SL, sample ID: NC1978; West Pacific, Coral Sea, E off New Caledonia, stn CP5126; 20°53.4′ S, 165°32.8′ E; 427–468 m deep; 30 Jun. 2021; RV *ALIS*; French beam trawl; SPANBIOS exped.; GenBank nos: OR261059 (*COI*), OR257540 (*cytb*), OR260575 (*rhodopsin*), OR257553 (*RAG1*); Voucher: NTUM17682 • 121.0 mm SL; West Pacific, Coral Sea, E off New Caledonia, "au large passe Yaté", stn CP3834; 22°06′ S, 167°04′ E; 257–258 m deep; 9 Sep. 2011; EXBODI exped.; Voucher: ASIZP73490 • 235.0 mm SL; West Pacific, Coral Sea, E off New Caledonia, "au large passe de la Sarcelles", stn CP3844; 22°20′ S, 167°22′ E; 815–970 m deep; 10 Sep. 2011; Voucher: ASIZP73491.

Description

Adult

Measurements and meristic counts. Morphometric values given in Tables 3 and 4. Dorsal-fin spines 6; dorsal-fin rays 8; anal-fin rays 6; pectoral-fin rays 23–24; pelvic-fin rays 7; branchiostegal rays 5;

quadrate spine 1; interopercular spines 2; vertebrae 18; outermost row of premaxillary teeth 12–27 (Tables 5–6).

Head and body. Head relatively short (28.4%–32.7% of SL, mean 29.8 ± 0.02%) and wide (58.1%–68.6% of HL, mean 63.2 ± 0.04%); eyes suboval; anterior half of premaxilla with three rows of enlarged teeth, largest on innermost row, followed by single row of small teeth on posterior half; maxilla toothless; palatine with single row of small teeth with some enlarged; dentary with three rows of teeth, outer teeth minute and innermost teeth largest; fifth ceratobranchial with two rows of small teeth, forming V-shaped patch; teeth on second and third pharyngobranchials forming small and rounded patches; gill rakers and pseudobranch absent. Palatine spines sharp, with posterior one stronger; frontal ridges and outer surface of maxilla bones bearing low and conical knobs; frontal spines blunt, with posterior one sharper and stronger; inner sphenotic spines low and blunt; outer sphenotic spines blunt; pterotic spines broad and blunt; parietal, epiotic, and posttemporal spines short and blunt, inconspicuous; articular spines strong and sharp, with single spine anterior to jaw joint and projected upward; quadrate spines strong and sharp; hyomandibular spines blunt; opercular spines blunt; interopercular spines blunt; subopercular spines sharp; cleithral spines strong and blunt; humeral spines well developed, with three to four sharp spinelets at its tip; edge of head and caudal peduncle covered by brown tendrils.

Fins. Illicium relatively long (24.6%–33.7% of SL, mean 27.9 ± 0.04%), without tendrils and extending beyond base of third dorsal spine; esca pennant-like flap without cirri or tassel-like flap with short cirri, sometimes with two dark, small, bulb-like appendages at base of esca; second dorsal-fin spine relatively long (19.7%–23.1% of SL, mean 21.9 ± 0.02%), stout, reaching base of third dorsal-fin spine, with dark tendrils; third dorsal-fin spine moderately long (19.3%–28.9% of SL, mean 23.8 ± 0.04%), slender, reaching base of retracted fourth dorsal-fin spine, base imbedded under skin, without tendrils; fourth dorsal-fin spine slender, about basal ⅓ imbedded under skin and with dark tendrils, reaching base of fifth dorsal-fin spine; fifth and sixth dorsal-fin spines short, mostly imbedded under skin and with dark tendrils; first dorsal-fin ray relatively close to second, both imbedded under skin, last two rays short; anterior three anal-fin rays imbedded under skin.

Coloration (preserved). Body color brown, covered by minute pale spots densely and irregular blackish-brown spots scarcely on dorsal surface; ventral surface pale, with peritoneum black; floor of mouth light with reticulate dark pattern; dorsal surface of pectoral-fins dark and pattern pigmented as adjacent area of body; dorsal-fin pale; caudal fin dark basally and apically, with pattern same as adjacent area of body.

Coloration (fresh). Body color khaki, covered by pale spot scarcely, blackish-brown reticulate marking and pigment spots on dorsal surface; dorsal surface of pectoral-fins blackish brown with pattern same as adjacent area of body basally; dorsal-fin pink; caudal fin dark basally and apically, tinged with pink, with pattern same as adjacent area of body.

Subdult

Unknown.

Distribution

Coral Sea, waters off New Caledonia at depths of 257–970 m (holotype and three adult paratypes); waters off eastern Australia at depths of 132–187 m (ten sequences from the BOLD systems) (this study, Fig. 1).

Remarks

Five specimens collected from the eastern Australian coast were examined by Caruso (1983: 13), suggesting that this new species might previously have been considered as an intraspecific variation of

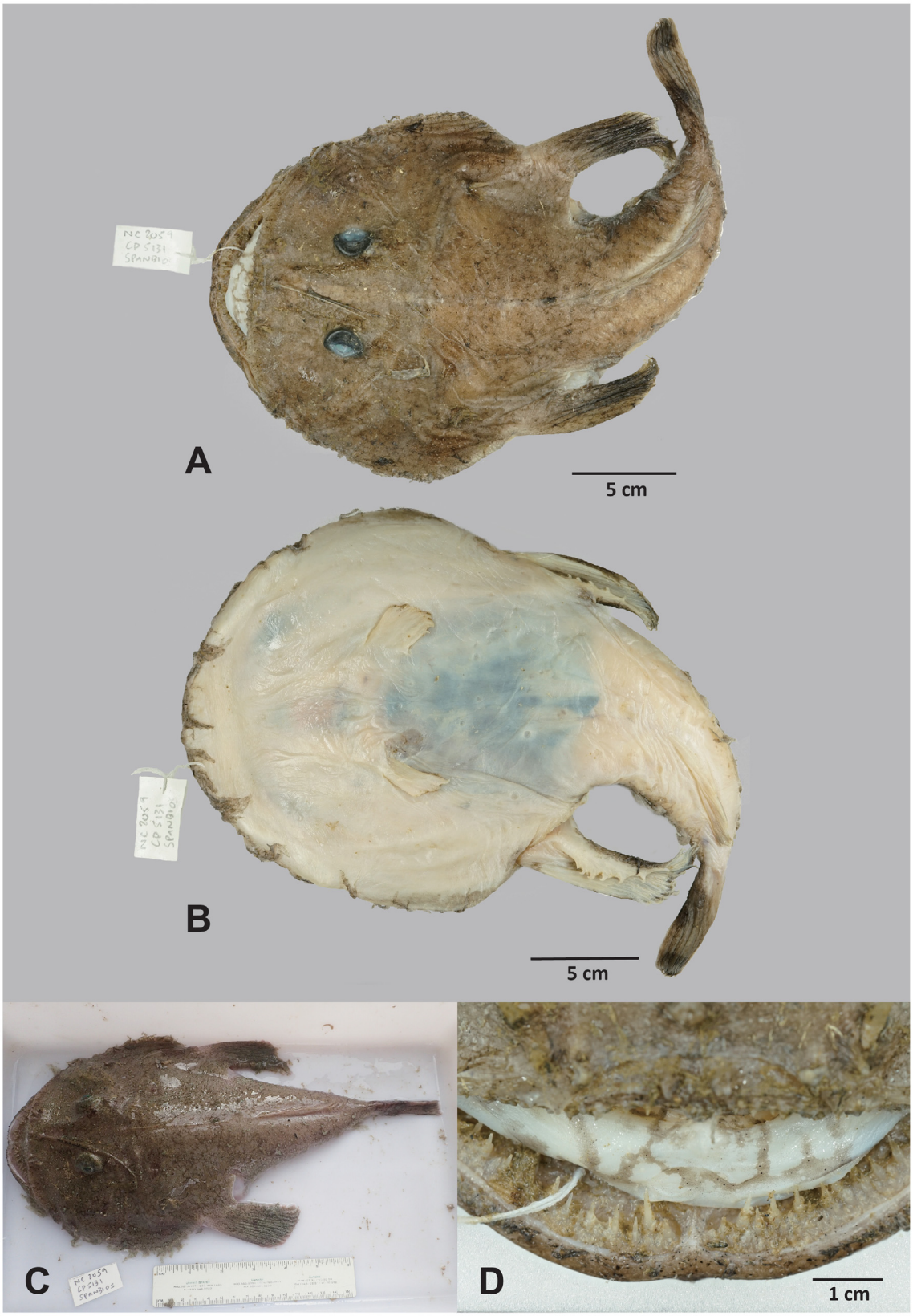

Fig. 14. *Lophiomus carusoi* sp. nov., holotype (MNHN 2024-0099, sample ID: NC2059). **A**. Preserved specimen, dorsal view. **B**. Ditto, ventral view. **C**. Fresh specimen. **D**. Preserved specimen, floor of mouth.

Lm. setigerus. Ten *COI* sequences initially identified as *Lm. setigerus*, obtained from the BOLD system, were reevaluated and considered to represent this new species. Photos of these samples (FOAN1063-11–FOAN1068-11), available on the BOLD systems, also demonstrate morphological similarities to this new species, particularly in terms of brown body coloration and the reticulate and dark pigmentation of the floor of the mouth, further supporting their conspecific status. Ho & Chen (2013) identified two specimens of *Lophiomus* (ASIZP73490 and ASIZP73491) collected from New Caledonia at depths of 815–970 m to be *Lm. setigerus*. However, the present morphological examination suggests that they should be *Lm. carusoi* sp. nov.

Keys

Key to the genera of Lophiidae

We revised couplet 3 of the key to the genera of Lophiidae provided by Caruso (1985):

3. Floor of mouth without any dark marking; outer surface of maxilla smooth; quadrate with two spines, both upper and lower spine present; interopercular spine with single spine; dorsal-fin rays 9–12; anal-fin rays 8–10; pectoral-fin rays 19–28; vertebrae 26–31 (Fig. 7B) ..... ***Lophius*** Linneaus, 1758
– Floor of mouth with conspicuous dark marking (except *Lm. immaculatus*), ranges from reticulate dark pattern, anastomosing dark pattern, to irregular or circular pale pattern on dark background; outer surface of maxilla bearing low conical knobs; quadrate with single lower spine; interopercular spine with two spines; dorsal-fin rays 8; anal-fin rays 6; pectoral-fin rays 21–25; vertebrae 18–19 (Figs 7C, 15) ..... ***Lophiomus*** Gill, 1883

Key to world species of *Lophiomus*

1. Floor of mouth without conspicuous dark marking (Fig. 12D); dorsal-fin spines 5; OPSOP less than 30% of HW ..... ***Lm. immaculioralis*** sp. nov.
– Floor of mouth with conspicuous dark markings (Figs 8D, H, 9C, G, 10C, 11D, H, 13D, H, 14D); dorsal-fin spines 6; OPSOP more than 30% of HW 2

2. Body color brown (Fig. 8A, C, E, G); floor of mouth with irregular or circular pale pattern on dark background (Fig. 8D, H); pectoral-fin rays 21–23 (mostly 22, rarely 21 and 23) (Table 6) .... ***Lm. setigerus*** (Vahl, 1797)
– Body color brown or pale khaki (Figs 10–11, 13); the floor of mouth not as above; pectoral-fin rays not less than 23 3

3. Peritoneum light (Fig. 9); floor of mouth with anastomosing dark patterns in the middle (Figs 10C, 11D, H); pectoral-fin rays 24–25; pelvic-fin rays 7 ..... ***Lm. laticeps*** (Ogilby, 1910) stat. rev.
– Peritoneum black (at least in adults) (Figs 13B, 14B); floor of mouth with reticulate pattern (Figs 13D, H, 14D); pectoral-fin rays 23–24; pelvic-fin rays 6 or 7 4

4. Body color pale khaki (Fig. 13A, C, E, G); esca pennant-like flap without cirri (Fig. 16C); pelvic-fin rays 6; DS4 8.4–17.3% of the SL; SNW 31.8–39.5%, ISP 40.6–45.4%, OPSOP 47.3–53.6% of the HL ..... ***Lm. nigriventris*** sp. nov.
– Body color brown (Fig. 14A–B); esca tassel-like or pennant-like flap with moderately long cirri (Fig. 16E–F); pelvic-fin rays 7; DS4 16.7–24.0% of the SL; SNW 41.9–55.7%, ISP 48.6–56.7%, OPSOP 55.5–65.7% of the HL ..... ***Lm. carusoi*** sp. nov.

Discussion

Our species delimitation results with multiline evidence suggests a six-fold increase in species richness in the genus *Lophiomus*. The description of *Lm. setigerus* sensu Caruso (1983) shows a wide range in

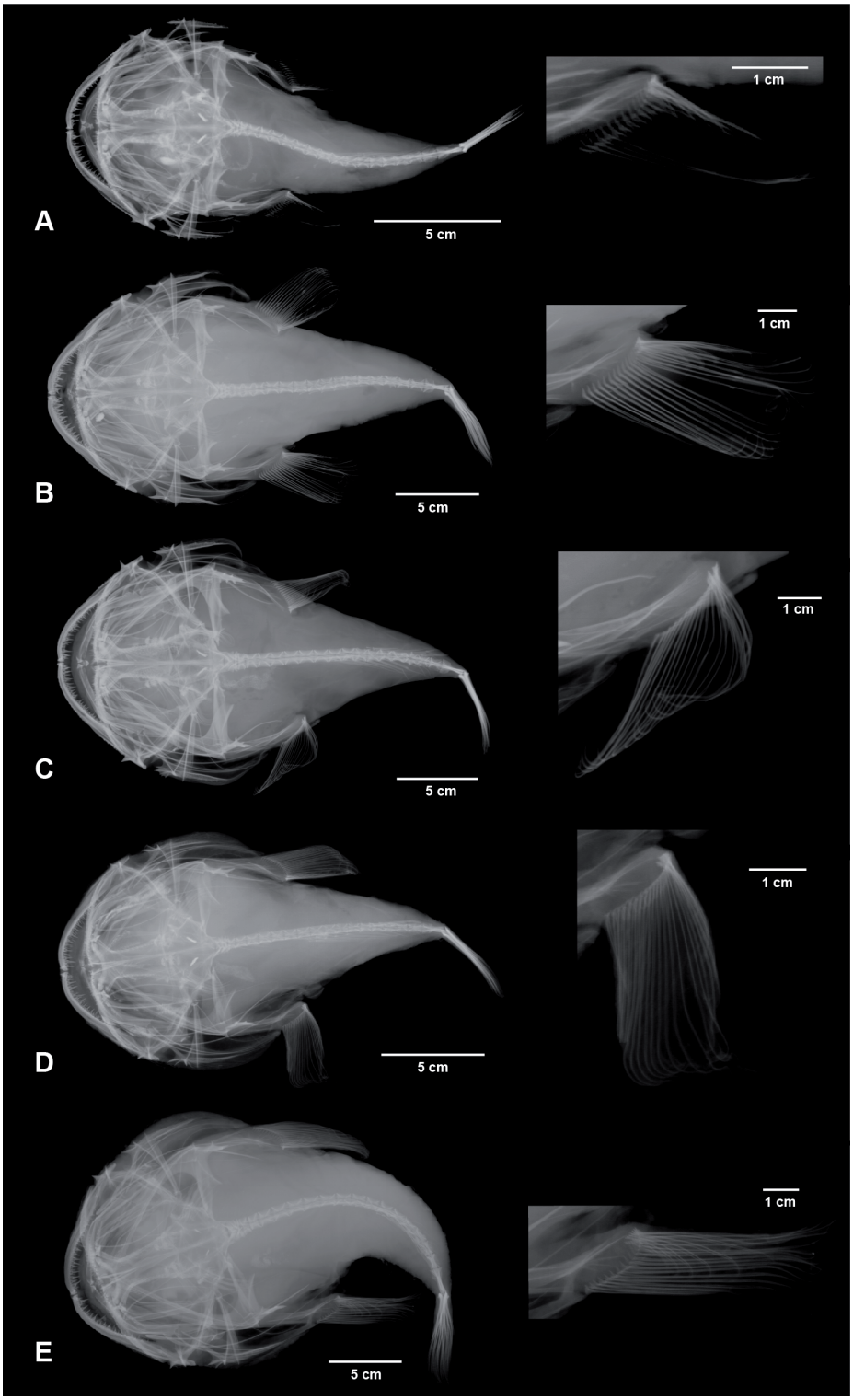

Fig. 15. X-ray radiographs in dorsal view and zoom-in images of left pectoral-fin of *Lophiomus* spp. collected in this study for visualizing interspecific variations in pectoral-fin ray counts. **A**. *Lm. setigerus* (Vahl, 1797), neotype (NTUM10408, sample ID: WJC0905). **B**. *Lm. laticeps* (Ogilby, 1910) stat. rev. (NTUM13463, sample ID: NC1375). **C**. *Lm. immaculioralis* sp. nov., holotype (NTUM16313, sample ID: WJC7777). **D**. *Lm. nigriventris* sp. nov., holotype (NTUM15096, sample ID: WJC5808). **E**. *Lm. carusoi* sp. nov., holotype (MNHN 2024-0099, sample ID: NC2059).

morphological variation: peritoneum pigmentation mostly gray but occasionally light or dark; dorsal body color ranging from light to dark brown; and 21–25 pectoral-fin rays. These variations encompass the currently described new species, indicating hidden diversity within the previously defined *Lm. setigerus*. *Lophiomus setigerus* was thought to be widespread in the IWP from South Africa in the west (Caruso 1986) to New Caledonia in the east (Kulbicki *et al.* 1994; Ho & Chen 2013). De La Cruz-Agüero *et al.* (1994) and Love *et al.* (2021) even reported *Lm. setigerus* found in Bahía Magdalena, Mexico. These records extend the known range of *Lm. setigerus* to the East Pacific. However, our

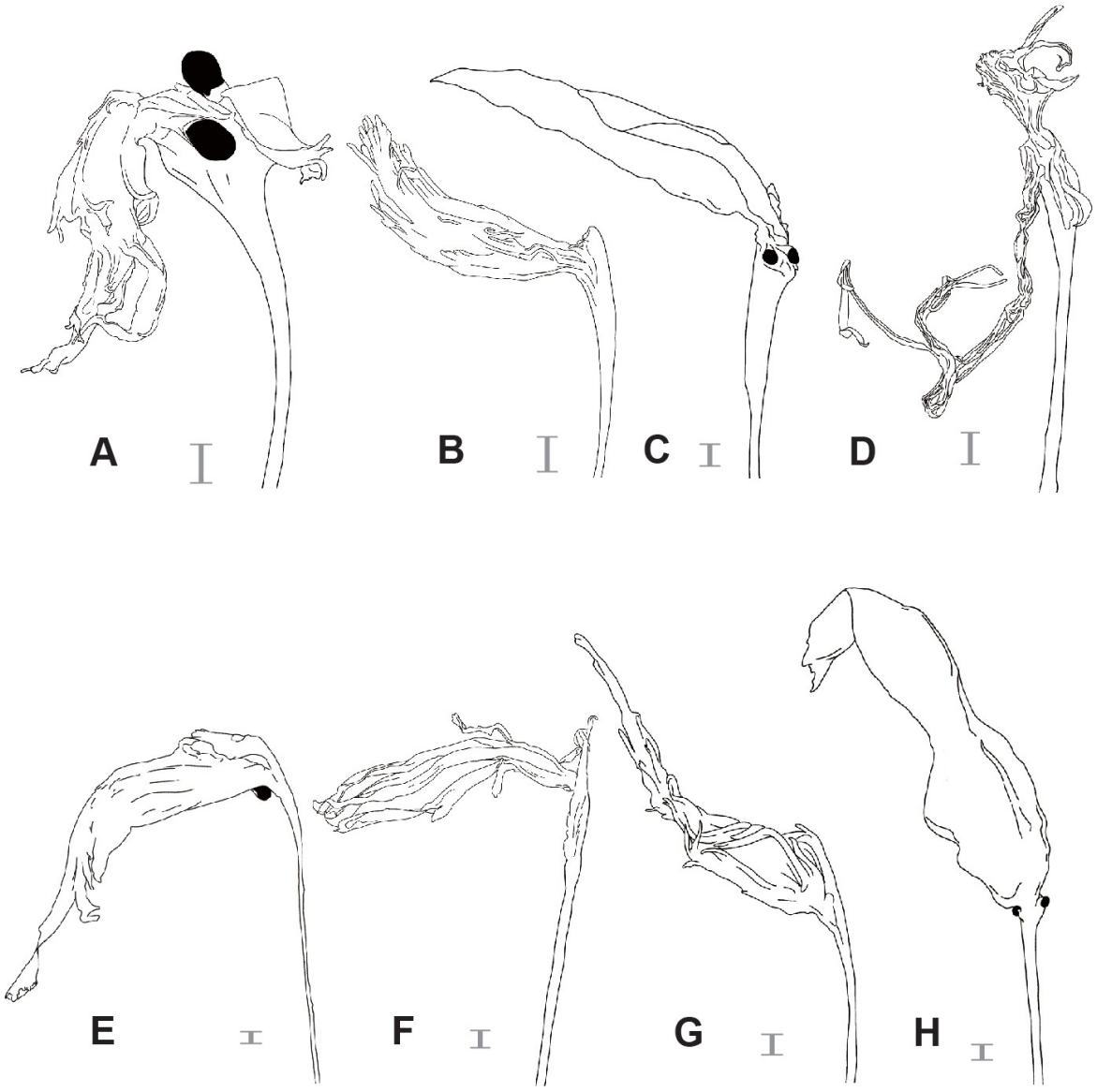

Fig. 16. Esca of *Lophiomus* spp. **A**. *Lm. laticeps* (Ogilby, 1910) stat. rev. (NTUM13463, sample ID: NC1375). **B**. Ditto (NTUM13468, sample ID: NC964). **C**. *Lm. nigriventris* sp. nov., holotype (NTUM15096, sample ID: WJC5808). **D**. *Lm. immaculioralis* sp. nov., holotype (NTUM16313, sample ID: WJC7777). **E**. *Lm. carusoi* sp. nov., holotype (MNHN 2024-0099, sample ID: NC2059). **F**. Ditto, paratype (NTUM17682, sample ID: NC1978). **G**. *Lm. setigerus* (Vahl, 1797) (NTUM14414, sample ID: WJC7223). **H**. Ditto (NTUM14414, sample ID: WJC7224). Scale bars = 1 mm.

molecule-based analyses suggest that the populations from eastern Australia (*Lm. carusoi* sp. nov. and *Lm. laticeps*) and India ('*Lp. indicus*') represent species different from *Lm. setigerus* (Fig. 2), and thus the distributional records for this species should be updated accordingly (Fig. 1). Due to a lack of sampling, the taxonomic status of the African and Mexican '*Lm. setigerus*' is not discussed herein and requires further confirmation.

Three previously described species, *C. laticeps* from eastern Australia off Queensland, *C. malabaricus* from southwestern India, and *Lp. indicus* from Bay of Bengal, were synonymized with *Lm. setigerus* by Caruso (1983). Our molecule-based results, along with a morphological comparison among newly collected specimens, the type series, and the original description of these synonyms, suggest the resurrection of *C. laticeps* to *Lm. laticeps*. Additionally, since the morphological differences are remarkable (see taxonomic remarks on *Lm. setigerus*), *C. malabaricus* could be a distinct species from *Lm. setigerus* as well. From our phylogenetic analysis, the three *COI* sequences labeled as '*Lp. indicus*' available in GenBank (sample locality: southwestern India; K.K. Bineesh pers. com.; Fig. 1) form an independent lineage within *Lophiomus* (Fig. 2). Its mean genetic divergence at *COI* to other congeners is large (>13%), implying its status as a separate species (Table 7). However, the voucher specimens for these '*Lp. indicus*' sequences are unavailable in this study, and the locality of the concerned samples is close to the type locality of *C. malabaricus* (Fig. 1; Table 1). Therefore, these sequences may actually correspond to *C. malabaricus* rather than *Lp. indicus*. Although the present evidence suggests *C. malabaricus* should be valid and its taxonomic status requires further revision, to be conservative we tentatively treat this nominal species as incertae sedis. Formal decision can be made after a throughout examination of type specimens and additional samples.

On the other hand, our genetic and morphological analyses reveal that *Lm. immaculioralis* sp. nov. is a new species of *Lophiomus* found in the Indian Ocean. Although the genetic distance of this species from *Lm. setigerus* is relatively low (K2P distance = 0.0513 at *COI* and 0.0528 at *cytb*) compared to those estimated from other species pairs (Table 7), it is higher than the average 3.5% of *COI* sequence divergence for sibling species of marine fishes found in the IWP region (Ward 2009; Zemlak *et al.* 2009). Conversely, our *COI* data reveal only a limited genetic divergence (2.34%) between the eastern Australian and New Caledonian populations of *Lm. carusoi* (Table 7). The difference in depth distributions of the two populations (132–196 m vs 354–468 m; Figs 1–2) suggests potential ecological niche partitioning and thus complete speciation. It is worth noting that the two additionally examined specimens (ASIZP73490 and ASIZP73491) of the New Caledonian *Lm. carusoi* were found to have been collected between, or at even greater depths (257–258 m and 815–970 m), than those of the other *Lm. carusoi* individuals sampled for genetic analysis, including those from eastern Australia (samples from BOLD systems). This finding suggests that *Lm. carusoi* has a wider depth distribution, so depth alone may not be a reliable criterion to separate *Lm. carusoi* into multiple OTUs or species. Further evidence, especially from population genetic analyses, is still required to evaluate the degree of gene flow between these two geographically separated populations. Here, we tentatively consider them to represent a single species.

Regarding inter-generic difference, our CT scanning results support the generic definition of Caruso (1983, 1985), which states that frontal ridge and maxillary bone morphology serve as reliable diagnostic characters for three lophiid genera: *Lophius*, *Lophiodes*, and *Lophiomus*. PCA and CVA results indicating potential diagnostic characters for *Lophiomus* species also partially support our morphological findings. For example, the percentages of HL and DS3 in the SL; HW, SNW, ISP, and OPSOP in the HL; and the meristic counts of pectoral- and pelvic-fin rays are useful in distinguishing among *Lophiomus* species to some extent. Finally, based on our current materials, the pattern of the floor of mouth appears to be an effective diagnostic character at the species level. However, it is important to note that more material and further studies are necessary to fully understand its infraspecific variation and uncover the biological significance of these floor of mouth patterns.

Acknowledgements

We would like to express our sincere thanks to the participants of the oceanography expeditions AURORA 2007, EXBODI (https://doi.org/10.17600/11100080), KAVIENG 2014 (https://doi.org/10.17600/14004400), ZHONGSHA 2015 (NSC 102-2923-B-002-001-MY3), KANADEEP 1 (inventory number: MNHN + APA-NC7; https://doi.org/10.17600/17003800), and SPANBIOS (inventory number: MNHN + APA-NC25; https://doi.org/10.17600/18000701), and the leaders and crews of R/V *DA-BFAR*, *ALIS*, and *ORI* in organizing the survey and collecting the samples under the *TDSB* and *TFDeepEvo* programs. We thank J. Maclaine and L. Goodayle (NHMUK), and A. Hay and K. Parkinson (AMS) for providing the excellent quality of photos/radiographs of the type specimens of *Lophius indicus* and *Chirolophius laticeps*; K.K. Bineesh, K.V. Akhilesh, and A. Gopalakrishnan (Central Marine Fisheries Research Institute, India) for providing the locality information of the '*Lophius indicus*' sequences in GenBank. We deeply appreciate the assistance received from H.-C. Michelle Lin (NTUM and Institute of Oceanography, National Taiwan University (IO NTU)) and S.-P. Huang (ASIZP) during specimen examination, the X-ray support from P. Tongboonkua and C.-C. Su lab members (IO NTU), the CT scanning support from C.-I. Lin (TIRI) and J.-J. Steven Huang (IO NTU), and the English editing of B. Pruitt. We also thank editor, Dr F. Ottoni, and four anonymous reviewers for providing helpful comments on this article. This study was supported by research funding from the National Science and Technology Council, Taiwan (NSTC) (102-2923-B-002-001-MY3, 110-2611-M-002-013, 111-2611-M-002-025, and 112-2611-M-002-025 to W.-J. Chen) and the French National Research Agency (ANR 12-ISV7-0005-01 to S. Samadi).

References

Alcock A.W. 1889. Natural history notes from H.M.'s Indian marine survey steamer '*Investigator*' no. 12. Descriptions of some new and rare species of fishes from the Bay of Bengal, obtained during the season of 1888–89. *Journal of the Asiatic Society of Bengal* 3: 296–305.

Bannikov A.F. 2004. The first discovery of an anglerfish (Teleostei, Lophiidae) in the Eocene of the Northern Caucasus. *Paleontological Journal* 38: 67–72.

Bianchi G. 1985. *Field Guide to the Commercial Marine and Brackish-water Species of Tanzania*. FAO FAO Species Identification Field Guide for Fishery Purposes, Rome.

Blender Foundation Community. 2018. Blender — A 3D modelling and rendering package. Available from https://www.blender.org [accessed 19 Mar. 2023].

Bloch M.E. & Schneider J.G. 1801. *M.E. Blochii, Systema Ichthyologiae Iconibus cx Ilustratum*. Sumtibus auctoris impressum et Bibliopolio Sanderiano commissum, Berlin [Berolini]. https://doi.org/10.5962/bhl.title.5750

Borsa P., Hsiao D.-R., Carpenter K.E. & Chen W.-J. 2013a. Cranial morphometrics and mitochondrial DNA sequences distinguish cryptic species of the longface emperor (*Lethrinus olivaceus*), an emblematic fish of Indo-west pacific coral reefs. *Comptes Rendus. Biologies* 336 (10): 505–514. https://doi.org/10.1016/j.crvi.2013.09.004

Borsa P., Arlyza I.S., Chen W.-J., Durand J.-D., Meekan M.G. & Shen K.-N. 2013b. Resurrection of New Caledonian maskray *Neotrygon trigonoides* (Myliobatoidei: Dasyatidae) from synonymy with *N. kuhlii*, based on cytochrome-oxidase I gene sequences and spotting patterns. *Comptes Rendus. Biologies* 336 (4): 221–232. https://doi.org/10.1016/j.crvi.2013.05.005

Borsa P., Sembiring A., Fauvelot C. & Chen W.-J. 2014. Resurrection of Indian Ocean humbug damselfish, *Dascyllus abudafur* (Forsskål) from synonymy with its Pacific Ocean sibling, *Dascyllus aruanus* (L.). *Comptes Rendus. Biologies* 337 (12): 709–716. https://doi.org/10.1016/j.crvi.2014.09.001

Bouchet P., Héros V., Lozouet P. & Maestrati P. 2008. A quarter-century of deep-sea malacological exploration in the south and West Pacific: where do we stand? How far to go. *In*: Héros V., Cowie R.H. & Bouchet P. (eds) *Tropical Deep-sea Benthos* 25: 9–40. Muséum national d'Histoire naturelle, Paris.

Carnevale G. & Pietsch T.W. 2012. †*Caruso*, a new genus of anglerfishes from the Eocene of Monte Bolca, Italy, with a comparative osteology and phylogeny of the teleost family lophiidae. *Journal of Systematic Palaeontology* 10 (1): 47–72. https://doi.org/10.1080/14772019.2011.565083

Caruso J.H. 1981. The systematics and distribution of the lophiid anglerfishes: I. A revision of the genus *Lophiodes* with the description of two new species. *Copeia* 1981 (3): 522–549. https://doi.org/10.2307/1444556

Caruso J.H. 1983. The systematics and distribution of the lophiid anglerfishes: II. Revisions of the genera *Lophiomus* and *Lophius*. *Copeia* 1983 (1): 11–30. https://doi.org/10.2307/1444694

Caruso J.H. 1985. The systematics and distribution of the lophiid anglerfishes: III. Intergeneric relationships. *Copeia* 1985 (4): 870–875. https://doi.org/10.2307/1445235

Caruso J.H. 1986. Lophiidae. *In*: Smith M.M. & Heemstra P.C. (eds) *Smiths' Sea Fishes*: 363–366. Springer-Verlag, Berlin.

Chen W.-J. & Borsa P. 2020. Diversity, phylogeny, and historical biogeography of large-eye seabreams (Teleostei: Lethrinidae). *Molecular Phylogenetics and Evolution* 151: e106902. https://doi.org/10.1016/j.ympev.2020.106902

Dayrat B. 2005. Towards integrative taxonomy. *Biological Journal of the Linnean society* 85 (3): 407–417. https://doi.org/10.1111/j.1095-8312.2005.00503.x

De la Cruz-Agüero J., Galván-Magaña F., Abitia-Cárdenas L.A., Rodríguez-Romero J. & Gutiérrez-Sánchez F.J. 1994. Systematic list of marine fishes from Bahia Magdalena, Baja California Sur (Mexico). *Ciencias Marinas* 20: 17–31. https://doi.org/10.7773/cm.v20i1.956

Fischer W., Sousa I., Silva C., de Freitas A., Poutiers J.M., Schneider W., Borges T.C., Feral J.P. & Massinga A. 1990. *Guia de Campo das Espécies comerciais marinhas e de Águas salobras de Moçambique*. Fichas FAO de Identificaçao de Espécies para Actividades de Pesca, Rome.

Fricke R., Eschmeyer W.N. & van der Laan R. 2022. Eschmeyer's Catalog of Fishes: Genera, Species, References.
Available from https://researcharchive.calacademy.org/research/ichthyology/catalog/fishcatmain.asp [accessed 23 Apr. 2023].

Gill T.N. 1883. Supplementary note on the Pediculati. *Proceedings of the United States National Museum* 5: 551–556. Available from https://www.biodiversitylibrary.org/page/7321063 [accessed 23 Apr. 2023].

Golani D. & Bogorodsky S.V. 2010. The fishes of the Red Sea — Reappraisal and updated checklist. *Zootaxa* 2463: 1–135. https://doi.org/10.11646/zootaxa.2463.1.1

Guindon S., Dufayard J.-F., Lefort V., Anisimova M., Hordijk W. & Gascuel O. 2010. New algorithms and methods to estimate maximum-likelihood phylogenies: assessing the performance of PhyML 3.0 *Systematic Biology* 59 (3): 307–321. https://doi.org/10.1093/sysbio/syq010

Haring P. & Maguire J. 2008. The monkfish fishery and its management in the northeastern USA. *ICES Journal of Marine Science* 65 (7): 1370–1379. https://doi.org/10.1093/icesjms/fsn131

Ho H.-C. & Chen W.-J. 2013. DNA sequences and morphological variation in *Lophiodes iwamotoi* Ho, Serét & Shao, 2011 based on new material from New Caledonia. *Zootaxa* 3682: 594–598. https://doi.org/10.11646/zootaxa.3682.4.12

Ho H.-C., Séret B. & Shao K.-T. 2011. Records of anglerfishes (Lophiiformes: Lophiidae) from the western South Pacific Ocean, with descriptions of two new species. *Journal of Fish Biology* 79: 1722–1745. https://doi.org/10.1111/j.1095-8649.2011.03106.x

Ho H.-C., Bineesh K.K. & Akhilesh K.V. 2014. Rediscovery of *Lophiodes triradiatus* (Lloyd, 1909), a senior synonym of *L. infrabrunneus* Smith and Radcliffe (Lophiiformes: Lophiidae). *Zootaxa* 3786: 587–592. https://doi.org/10.11646/zootaxa.3786.5.6

Hoang D.T., Chernomor O., von Haeseler A., Minh B.Q. & Vinh L.S. 2017. UFboot2: Improving the Ultrafast Bootstrap Approximation. *Molecular Biology and Evolution* 35 (2): 518–522. https://doi.org/10.1093/molbev/msx281

Huang C.-S. 2015. *Molecular Systematics of the Lophiidae, Ogcocephalidae, and Chaunacidae (Lophiiformes) occurring in Western Pacific Ocean*. Master thesis, National Taiwan University.

Hung K.-W., Russell B.C. & Chen W.-J. 2017. Molecular systematics of threadfin breams and relatives (Teleostei, Nemipteridae). *Zoologica Scripta* 46 (5): 536–551. https://doi.org/10.1111/zsc.12237

Ivanova N., Zemlak T., Hanner R. & Hebert P. 2007. Universal primer cocktails for fish DNA barcoding. *Molecular Ecology Notes* 7 (4): 544–548. https://doi.org/10.1111/j.1471-8286.2007.01748.x

Kalyaanamoorthy S., Minh B.Q., Wong T.K.F., von Haeseler A. & Jermiin L.S. 2017. Modelfinder: Fast model selection for accurate phylogenetic estimates. *Nature Methods* 14: 587–589. https://doi.org/10.1038/nmeth.4285

Katoh K., Rozewicki J. & Yamada K.D. 2019. MAFFT online service: Multiple sequence alignment, interactive sequence choice and visualization. *Briefings in Bioinformatics* 20 (4): 1160–1166. https://doi.org/10.1093/bib/bbx108

Kekkonen M. & Hebert P.D. 2014. DNA barcode-based delineation of putative species: efficient start for taxonomic workflows. *Molecular Ecology Resources* 14 (4): 706–715. https://doi.org/10.1111/1755-0998.12233

Khalaf M.A. 2004. Fish fauna of the Jordanian Coast, Gulf of Aqaba, Red Sea. *Journal of King Abdulaziz University: Marine Sciences* 15 (1): 23–50.

Kikinis R., Pieper S.D. & Vosburgh K.G. 2014. 3D Slicer: A platform for subject-specific image analysis, visualization, and clinical support. *In*: Jolesz F. (ed.) *Intraoperative Imaging and Image-Guided Therapy*: 277–289. Springer, New York, NY. https://doi.org/10.1007/978-1-4614-7657-3_19

Kulbicki M., Randall J.E. & Rivaton J. 1994. Checklist of the fishes of the Chesterfield islands (Coral Sea). *Micronesica* 27: 1–43.

Lee S.-H., Lee M.-Y., Matsunuma M. & Chen W.-J. 2019. Exploring the phylogeny and species diversity of *Chelidoperca* (Teleostei: Serranidae) from the western Pacific Ocean by an integrated approach in systematics, with descriptions of three new species and a redescription of *C. lecromi* Fourmanoir, 1982. *Frontiers in Marine Science* 6: 1–26. https://doi.org/10.3389/fmars.2019.00465

Leslie R.W. & Grant W.S. 1991. Redescription of the Southern African Anglerfish *Lophius vomerinus* Valenciennes, 1837 (Lophiiformes: Lophiidae). *Copeia* 1991 (3): 787–800. https://doi.org/10.2307/1446406

Lo P.C., Liu S.H., Nor S.A.M. & Chen W.-J. 2017. Molecular exploration of hidden diversity in the Indo-West Pacific sciaenid clade. *PLoS ONE* 12 (7): e0176623. https://doi.org/10.1371/journal.pone.0176623

Love M.S., Bizzarro J.J., Cornthwaite A.M., Frable B.W. & Maslenikov K.P. 2021. Checklist of marine and estuarine fishes from the Alaska–Yukon Border, Beaufort Sea, to Cabo San Lucas, Mexico. *Zootaxa* 5053 (1): 1–285. https://doi.org/10.11646/zootaxa.5053.1.1

Minh B.Q., Nguyen M.A.T. & von Haeseler A. 2013. Ultrafast approximation for phylogenetic bootstrap. *Molecular Biology and Evolution* 30 (5): 1188–1195. https://doi.org/10.1093/molbev/mst024

Minh B.Q., Schmidt H.A., Chernomor O., Schrempf D., Woodhams M.D., von Haeseler A. & Lanfear R. 2020. IQ-TREE 2: New models and efficient methods for phylogenetic inference in the genomic era. *Molecular Biology and Evolution* 37 (5): 1530–1534. https://doi.org/10.1093/molbev/msaa015

Miya M., Pietsch T.W., Orr J.W., Arnold R.J., Satoh T.P., Shedlock A.M. Ho H.-C., Shimazaki M., Yabe M. & Nishida M. 2010. Evolutionary history of anglerfishes (Teleostei: Lophiiformes): a mitogenomic perspective. *BMC Evolutionary Biology* 10: 1–27. https://doi.org/10.1186/1471-2148-10-58

Ni Y., Wu H.-L. & Li S. 2012. A new species of the genus *Sladenia* (Pisces, Lophiidae) from the East China Sea and South China Sea. *Acta Zootaxonomica Sinica* 37 (1): 211–216.

Ogilby J.D. 1910. On some new fishes from the Queensland coast. Endeavour Series, No. 1. *The Proceedings of the Royal Society of Queensland* 23: 85–139. https://doi.org/10.5962/p.351378

Pietsch T. 1984. Lophiiformes: Development and relationships. *In*: Moser H. *et al.* (eds) *Ontogeny and Systematics of Fishes*. Special Publication 1: 320–325. American Society of Ichthyologists and Herpetologists, Lawrence, KS.

Pietsch T. 2009. *Oceanic Anglerfishes. Extraordinary Diversity in the Deep Sea*. University of California Press, Berkeley, CA. https://doi.org/10.1525/9780520942554

Pietsch T. & Carnevale G. 2011. A new genus and species of lophiid anglerfish (Teleostei: Lophiiformes) from the Eocene of Monte Bolca, Italy. *Copeia* 2011: 64–71. https://doi.org/10.1643/CI-10-080

Puillandre N., Brouillet S. & Achaz G. 2020. ASAP: assemble species by automatic partitioning. *Molecular Ecology Resources* 21 (2): 609–620. https://doi.org/10.1111/1755-0998.13281

Ratnasingham S. & Hebert P.D.N. 2007. BOLD: The Barcode of Life Data System (http://www.barcodinglife.org). *Molecular Ecology Notes* 7: 355–364. https://doi.org/10.1111/j.1471-8286.2007.01678.x

R Core Team. 2022. R: A language and environment for statistical computing. Ver. 4.2.1 Available from https://www.r-project.org/ [accessed 19 Mar. 2022].

Ronquist F., Teslenko M., van der Mark P., Ayres D.L., Darling A., Höhna S., Larget B., Liu L., Suchard M.A. & Huelsenbeck J.P. 2012. MrBayes 3.2: efficient Bayesian phylogenetic inference and model choice across a large model space. *Systematic Biology* 61 (3): 539–542. https://doi.org/10.1093/sysbio/sys029

Samuel C.T. 1963. Bottom fishes collected by R.V. *Conch* off the Kerala coast. *Bulletin of the Department of Marine Biology Oceanogrphy, University of Kerala* 1: 97–121.

Schindelin J., Arganda-Carreras I., Frise E., Kaynig V., Longair M., Pietzsch T., Prebisch S., Rueden C., Saalfeld S., Schmid B., Tinevez J.-Y., White D.J., Hartenstein V., Eliceiri K., Tomancak P. & Cardona A. 2012. Fiji: an open-source platform for biological-image analysis. *Nature Methods* 9: 676–682. https://doi.org/10.1038/nmeth.2019

Sommer C., Schneider W. & Poutiers J.-M. 1996. *The Living Marine Resources of Somalia*. FAO Species Identification Field Guide for Fishery Purposes, Rome.

Tamura K., Stecher G. & Kumar S. 2021. MEGA11: Molecular Evolutionary Genetics Analysis version 11. *Molecular Biology and Evolution* 38 (7): 3022–3027. https://doi.org/10.1093/molbev/msab120

Tanaka S. 1918. Twelve new species of Japanese fishes. *Dobutsugaku Zasshi* 30: 223–227.

Vahl M. 1797. Beskrivelse tvende nye arter af bredflab-slaegten *Lophius*. *Skrivter af Naturhistorie-Selskabet Kiøbenhavn* 4: 212–216. Available from https://www.biodiversitylibrary.org/page/58273971 [accessed 19 Mar. 2023].

Ward R.D. 2009. DNA barcode divergence among species and genera of birds and fishes. *Molecular Ecology Resources* 9: 1077–1085. https://doi.org/10.1111/j.1755-0998.2009.02541.x

Ward R.D., Zemlak T.S., Innes B.H., Last P.R. & Hebert P.D. 2005. DNA barcoding Australia's fish species. *Philosophical Transactions of the Royal Society B: Biological Sciences* 360 (1462): 1847–1857. https://doi.org/10.1098/rstb.2005.1716

Zemlak T.S., Ward R.D., Connell A.D., Holmes B.H. & Hebert P.D.N. 2009. DNA barcoding reveals overlooked marine fishes. *Molecular Ecology Resources* 9: 237–242. https://doi.org/10.1111/j.1755-0998.2009.02649.x

Zhang J., Kapli P., Pavlidis P. & Stamatakis A. 2013. A general species delimitation method with applications to phylogenetic placements. *Bioinformatics* 29 (22): 2869–2876. https://doi.org/10.1093/bioinformatics/btt499

Manuscript received: 10 January 2024
Manuscript accepted: 18 April 2024
Published on: 15 July 2024
Topic editor: Magalie Castelin
Section editor: Felipe Ottoni
Desk editor: Pepe Fernández

Supplementary files

Supp. file 1. The information of specimens and sequences used in this study. Table in .xlsx file.
https://doi.org/10.5852/ejt.2024.943.2599.11865

Supp. file 2. PCR primers used in this study. PCR conditions of all markers were in 35 cycles.
https://doi.org/10.5852/ejt.2024.943.2599.11867

Supp. file 3. Fasta files containing all markers and datasets analyzed in this study, along with the Nexus file specifically for the TC dataset used in Bayesian inference.
https://doi.org/10.5852/ejt.2024.943.2599.11869

Supp. file 4. Coefficients of first and second principal components (PC1 and PC2), and the scaling of first and second principals of linear discriminants (LD1 and LD2) for the canonical variant analysis. https://doi.org/10.5852/ejt.2024.943.2599.11871

Supp. file 5**.** 3D reconstruction of the lophiid skeletons analyzed through CT-scanning in this study, available in .stl files. https://doi.org/10.5852/ejt.2024.943.2599.11873
Link for downloading the file: https://www.dropbox.com/scl/fi/a990a9aepyq6it73l05rd/Supplementary-File-5-copy.zip?rlkey=vev98xvhn0w51wmh6d84693wx&dl=0